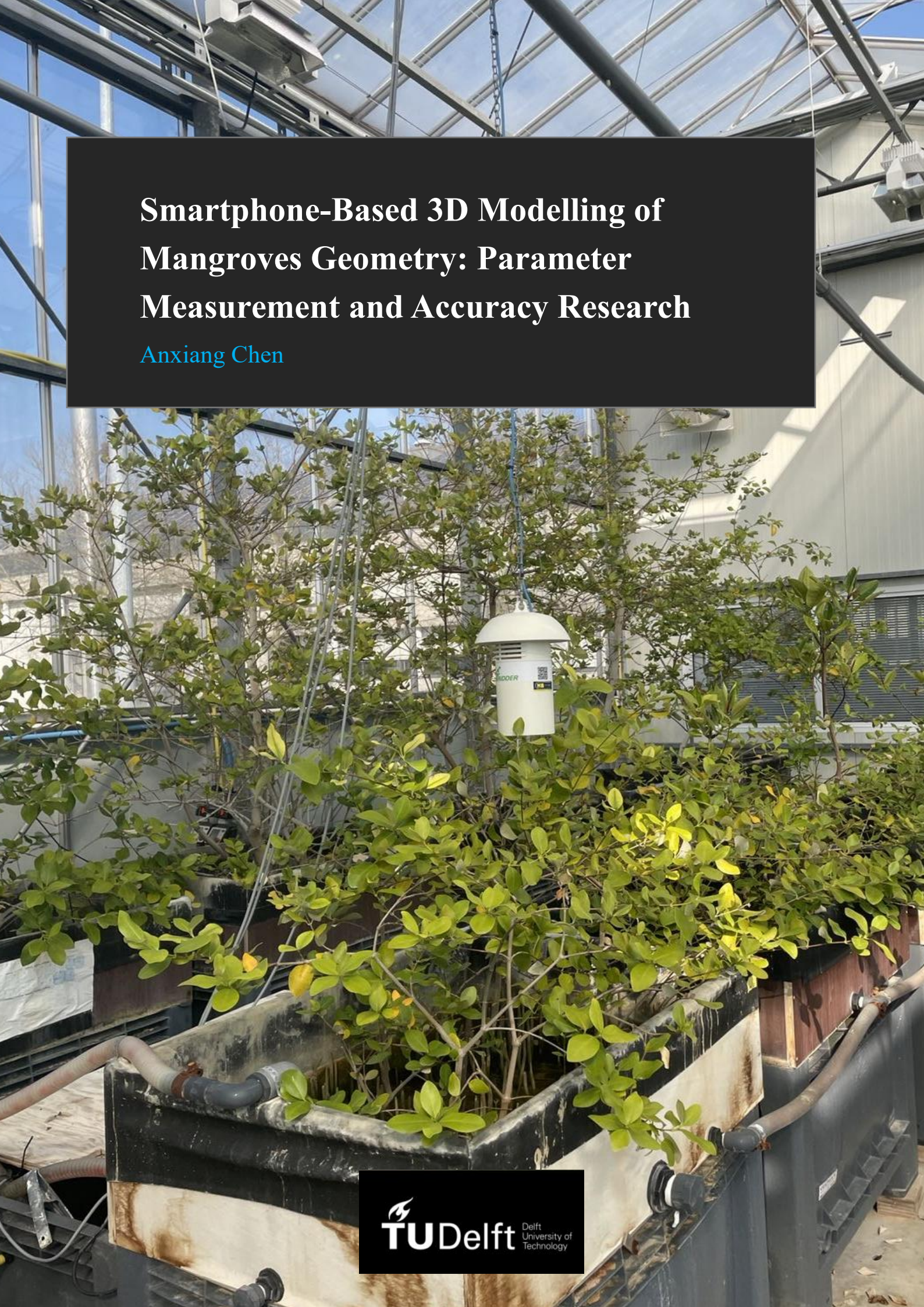

Smartphone-Based 3D Modelling of Mangroves Geometry: Parameter Measurement and Accuracy Research

Anxiang Chen

TU Delft Delft University of Technology

Smartphone-Based 3D Modelling of Mangroves Geometry: Parameter Measurement and Accuracy Research

by

Anxiang Chen

in partial fulfifillment of the requirements for the degree of

Master of Science

in Civil Engineering

at the Delft University of Technology,

to be defended on Tuesday November 15, 2022 at 11:00 AM.

Student number: 5254116

Project duration: March, 2022 – November, 2022

Thesis committee:

Dr. Ir. B. K. van Wesenbeeck	TU Delft & Deltares
Dr. Ir. B. Hofland	TU Delft
Ir. Su Kalloe	TU Delft
Dr. Ir. A.Gijon Mancheno	TU Delft

Cover: Mangroves growed in the Greenhouse at Deltares.

Abstract

The wave attenuation of vegetation plays an increasingly important role in flood control in coastal areas. Past studies have found that the interaction of waves with vegetation mainly depends on hydraulic conditions and vegetation characteristics. Therefore, it is necessary to build vegetation models and quantify vegetation characteristics related to wave attenuation. Mangroves are one of the typical tropical intertidal vegetation. This study aimed to test the potential of using a low-cost, convenient smartphone-based structure-from-motion with multi-view stereo-photogrammetry (SfM-MVS) to accurately measure mangrove parameters related to wave attenuation.

SfM-MVS is a computer vision technique in which the point cloud coordinates of an object can be calculated from a series of 2D photos to generate a 3D point cloud model. This study first tested the optimal photography distance (about 25cm) and optimal weather conditions (cloudy and no sunlight) using the smartphone-based SfM-MVS method. Then, based on the optiaml usage conditions, 3D point cloud models of 10 individual mangrove samples were reconstructed using this method, then the mangrove parameters related to wave attenuation were estimated according to the model: linear parameters (tree height, crown diameter, stem diameter, branches diameter) and the frontal area at a certain height. The true values of these parameters were measured using traditional hand measurements to evaluate smartphone-based SfM-MVS-derived parameter estimates.

The results show that the estimation of the linear parameters of the mangroves generally achieves high accuracy（$\mathrm{RMSE}_{\text{tree height}} = 13.51\%$, $\mathrm{RMSE}_{\text{canopy diameter}} = 11.28\%$, $\mathrm{RMSE}_{\text{stem diameter}} = 5.38\%$, $\mathrm{RMSE}_{\text{thicker branch diameter}} = 4.78\%$, $\mathrm{RMSE}_{\text{thinner branch diameter}} = 7.41\%$）.There were significant negative biases in the estimates of tree height and crown diameter, and no significant biases in the estimates of stems and branches. The results of linear regression show that there is a strong positive correlation between the estimated values of all parameters and the true values.There are large errors and negative biases in the estimates of the frontal area at different heights. Overall, $\mathrm{RMSE}_{\text{frontal area at a certain height}} = 45.58\%$ with a bias of -38.83%. This result showed that the SfM-MVS model resulted in a large underestimation of the frontal area at each height. A series of analyses showed that the main reason for the large error in the frontal area at a certain height was that the terminal branches with the lowest branch order (smallest diameter) were difficult to visualize in the SfM-MVS model. And this part of the branches actually occupies a large proportion of the frontal area.

This study demonstrates that smartphone-based SfM-MVS is capable of estimating mangrove tree height, canopy diameter, stem diameter, and thick branch diameter. Its accuracy is comparable to other existing methods such as TLS, ALS, camera-based SfM-MVS. However, the resolution is insufficient for very thin branches (<=5mm), which makes the method inaccurate in estimating the frontal area at a certain height. Factors such as photography distance and ambient lighting can affect the accuracy of the model. Compared with the currently used remote sensing technologies such as TLS, the smartphone-based SfM-MVS has the advantages of low cost, high flexibility, and

low difficulty for those who lack professional knowledge or training, which makes it an alternative with great potential. This method requires more testing and research in the future to improve its accuracy and practicality.

Preface

I am very fortunate that my master's career is more than enough to end with such a thesis. This marks the conclusion of my two-year study abroad career in the Netherlands. I have benefited a lot in the process of completing this thesis. I have always been passionate about the flood control of coastal vegetation and 3D modeling techniques. This graduation project gave me the opportunity to combine the two in research. I firmly believe that this technology has unlimited potential, it will make further progress in the future, and I hope my research can provide a useful foundation for future scholars. All in all, what I have learned and felt during my graduation project is something that I will use throughout my life, and I am very grateful for that.

First of all I want to thank the members of my graduation committee. Thanks to Bregje van Wesenbeeck for giving me this very meaningful opportunity for graduation project, and for giving me kind guidance and advice during this period. Thanks to Bas Hofland, his advice is very professional and allows me to spot problems and correct them in time every time. He is a teacher who is very rigorous and serious in academics but has a gentle heart. Thanks to Alejandra Gijón Mancheño and Su Kalloe, who as supervisors enthusiastically and carefully guided my entire graduation process. Alejandra is very careful to summarize the content of the meeting and give me a lot of useful daily information. Su followed my whole experimental process, analyzed and thought about many professional issues with me. It is my honor to meet such a graduation committee, with their help, I was able to complete my master's career so smoothly.

I would also like to thank my friends in the Netherlands, who were my greatest emotional sustenance during my study abroad. Thanks to my girlfriend Jialun Wu for giving me love and encouragement.

Anxiang Chen
Delft, October 2022

Content

Nomenclature

Abbreviations

SfM-MVS: Structure-from-motion with multi-view stereo-photogrammetry

TLS： Terrestrial laser scanning

ALS： Airborne Laser Scanning

RMSE： Root-mean-square-error

AE： Absolute error

Symbols

TH: Tree height	[m]
CD: Canopy diameter	[m]
SD: Stem diameter	[m]
BD1: Branch diameter (thicker)	[m]
BD2: Branch diameter (thinner)	[m]
FA: Frontal area	[m^2]
FA at a certain height: Frontal area at a certain height	[m]
L1: 1/5 of the tree height from bottom to top	[m]
L2: 2/5 of the tree height from bottom to top	[m]
L3: 3/5 of the tree height from bottom to top	[m]
L4: 4/5 of the tree height from bottom to top	[m]

1. Introduction

1.1. Problem description

Globally, approximately 600 million people are at risk of coastal flooding, of which 320 million are located in urban areas (McGranahan et al., 2007). Coastal communities are now facing increased flood risk due to more frequent disasters and the increase of population living on coastlines and floodplains (Douglas et al., 2008). Meanwhile, extreme sea-level rise and socioeconomic development will expose increasing numbers of people and assets to risk of coastal flooding in the future (van Zelst et al., 2021).

Nature-based solutions have great potential for adaptation and flood risk reduction (van Wesenbeeck et al., 2022). Among them, aquatic vegetation is known to be food and shelter for many organisms, and can control geobiochemical cycles in coastal areas, dissipate wave energy and turbulence, and protect coasts from erosion (Mendez et al., 2003). For example, in many tropical and subtropical regions, stable intertidal mudflats often support mangrove growth (Maza et al., 2021). Mangroves are well known for the numerous ecosystem services they can provide. Their dense vegetation and high intertidal elevation make them effective natural wave-attenuating structures (Horstman et al., 2014), and become the first line of protection against flooding and erosion (Menéndez et al., 2020). The roots of mangroves can retain sediment, stabilize soils in intertidal areas and reduce erosion (Tampanya et al., 2006). Roots, trunks and tree crowns can dissipate storm surges (Mcivor et al., 2012). Based on these observations, the ability of aquatic vegetation such as mangroves to attenuate waves and mitigate storm damage has received increasing attention (van Wesenbeeck et al., 2022). Quantifying the value of mangroves as natural coastal defenses is essential to incentivize conservation and restoration of mangroves for the benefit of nature and people (Hochard et al., 2019).

The basis for assessing the natural defense capabilities of intertidal ecosystems such as mangroves is to quantify the contribution of coastal vegetation to wave attenuation (Zhang et al., 2021). The attenuation of wave energy through aquatic vegetation is based on two processes: wave breaking and wave-vegetation interaction (Vo-Luong and Massel, 2008). And due to the structural complexity of vegetation and the unpredictability of hydrodynamic conditions, this wave attenuation is a highly variable process (Koch et al., 2009; Phan et al., 2019). The wave attenuation process is affected by vegetation characteristics and hydrodynamic conditions, among which the most relevant vegetation characteristics are vegetation density, height and geometry (Hu et al., 2014). Ysebaert et al. (2011) also believed that plant morphological characteristics are more influential than biomechanical characteristics in influencing wave resistance. Therefore, in order to further explore the role of vegetation in wave attenuation, quantifying the morphological vegetation characteristics is an important step. In fact, many studies have estimated the relationship between different characteristics of vegetation and its wave resistance. Among them,

important characteristics include vegetation age, plant density, tree height, canopy diameter, stem diameter, aboveground biomass and frontal area over the height, etc. (Maza et al., 2021; Kelty et al., 2022; Zhang et al., 2021; Paul et al., 2016; lou et al., 2018; Kalloe et al., 2022; Yin and Wang, 2019).

The ability to accurately obtain plant metrics is critical in several related fields (Miller et al., 2015). Traditional tree measurement methods (i.e. hand measurements) are not only time- and labor-intensive, but are also prone to errors because they do not guarantee the adequacy of measurements for more complex tree structures or larger trees (Bragg, 2008). A newer measure is the reconstruction of 3D models of trees (Miller et al., 2015). The three-dimensional reconstruction of trees is of great significance for representing the complex structure, geometric shape and spatial display of trees. Automatic 3D modeling of trees and branches is a necessary technique for effectively measuring tree characteristics (height, width, diameter, biomass, volume, etc.) and provides us with the means to visualize trees in virtual 3D space (Indirabai et al., 2019). Despite the geometric complexity of mangrove, numerical models usually simplify vegetation by representing it as a rigid cylinder (Suzuki et al., 2012). More accurate 3D models can provide high resolution data for numerical models, and will enable checking which simplifications do not compromise the modelling accuracy. This can be achieved by methods that produce accurate spatial point clouds, such as structure-from-motion with multi-view stereo-photogrammetry (SfM-MVS) (James et al., 2012)， Terrestrial Laser Sensors (TLS) (Kankare et al., 2013) and Airborne Laser Scanning (ALS) (Maltamo et al., 2014). Based on the accurate spatial point cloud, some important parameters related to wave attenuation, such as vegetation frontal area, can be obtained by some methods of extracting 2D parameters from 3D point cloud models (e.g., Kalloe et al., 2022).

Traditional photogrammetry requires the presence of a series of identifiable points in at least two photographs, and also requires that the image projection and camera position, orientation and distortion are known (Robertson and Cipolla, 2009). While SfM (Structure-from-Motion) is a valuable new tool for generating 3D models from 2D images (Szeliski, 2010). In SfM, a series of algorithms are used to identify repeating features in a collection of images, and then calculate the camera position and orientation based on the differential positions of these repeating features (Fisher et al., 2005, Szeliski, 2010). Based on this, some images with overlapping areas can be used to reconstruct a 3D model of the subject. The Multi-View Stereo (MVS) algorithm is then used to generate additional points to create a denser point cloud. This workflow is called SfM-MVS (Smith et al., 2016).

In addition to SfM-MVS, the development of Airborne Laser Scanning (ALS) and Terrestrial Laser Sensors (TLS) over the past decade has allowed us to find that these modern techniques can extract tree properties at finer scales (Marchi et al., 2018). Typical Airborne Laser Scanning (ALS) is commonly used to measure specific tree tops, obtain tree height or canopy dimensions, and predict features of interest through a set of allometric models (Maltamo et al., 2014). Terrestrial Lidar can provide detailed, objective, three-dimensional precise indicators of tree structure (Indirabai et al., 2019). It is obvious that modern technologies such as ALS and TLS are more

efficient, more accurate, and has more potential than traditional manual measurement methods for obtaining vegetation characteristic parameters (Kankare et al., 2013; Novotny et al., 2021).

Meanwhile, as technology advances rapidly, significant advances of smartphones and tablets in built-in sensors (especially cameras), available computing power, and onboard memory are transforming the role of these devices into critical digital platforms for fieldwork (Corradetti et al., 2021; Tavani et al., 2022). To the authors knowledge, few studies have used smartphone-based structure-from-motion with multi-view stereo-photogrammetry (SfM-MVS) for feature assessment and parameter acquisition of mangroves. While the methods such as terrestrial laser scanning and remote sensing drones used in most studies are often expensive and inconvenient to operate. For example, using a large terrestrial laser system in a mangrove forest would be costly and heavily influenced by the often soft and waterlogged ground and high forest density. If hand-held laser scanners or drones are used, in addition to the higher cost, they are also difficult to operate and inconvenient to carry. However, if a smartphone can be used to scan and model mangroves in the field with the required accuracy, it can save a lot of time and economic costs and adapt to flexible operations in the field.

Therefore, this study will use the smartphone-based SfM-MVS method to obtain the individual characteristic parameters of mangroves related to wave attenuation, explore the applicable conditions of the smartphone-based tree 3D modeling method and looking for factors that affect its accuracy. So as contributes to the more efficient study of the flood control characteristics of vegetation such as mangroves.

1.2. Research scope and research questions

The purpose of this study is to explore the feasibility of smartphone-based structure-from-motion with multi-view stereo-photogrammetry (SfM-MVS) for obtaining mangrove parameters related to wave damping, focus on the optimal conditions for reconstructing mangrove model using this method and the accuracy of parameters estimation, so as to better study the flood control characteristics of mangroves.

1.2.1. Research question

Main research question:
Is it feasible to determine relevant mangrove parameters for wave damping using a smartphone-based SfM-MVS approach?

To be able to answer this question, the following sub-questions are formulated:

1. What are the relevant mangrove parameters for wave damping?
2. How to use smartphone-based SfM-MVS to obtain the parameters?

3. What is the optimal condition to use smartphone-based SfM-MVS for mangrove ?
4. What is the accuracy of the mangrove parameter estimates using this method?
5. What factors could affect the accuracy of mangrove parameter estimates using this method?
6. How to correct and improve this technique?

1.3. Research approach and outline

In order to clarify the main research questions raised in the previous section, this study will reconstruct the 3D model of the mangrove individual through smartphone application, and then obtain the mangrove parameters in the 3D point cloud analysis software. The results of manual measurements in the field are considered "true values" to verify the accuracy of the method. The specific process is shown in Figure 1.2.

The mangrove samples used in this study were all of the same mangrove species grown in the greenhouse in Deltares, the Netherlands. The specific process of the smartphone-based SfM-MVS is as follows: First, use the mobile phone 3D modeling software to reconstruct the 3D model of the target mangrove individual. The resulting 3D model is then imported into point cloud analysis software in point cloud format. Through point cloud processing and ranging tools, the required mangrove parameters are obtained. At the same time as the reconstruction of the mangrove 3D model, the "true values" of the mangrove parameters were obtained by hand-measurement. The mangrove parameters obtained by smartphone-based SfM-MVS were compared with the "true values" to determine the accuracy of the method.

For the same mangrove sample, the control variable method was used to vary the photography distance and environmental conditions. The optimal usage conditions of the smartphone-based SfM-MVS method were determined according to the obtained parameter error values. Based on this optimal use condition, the performance and decision factors of the smartphone-based SfM-MVS method in measuring the parameters related to wave damping in mangroves are determined.

The research questions mentioned in Section 1.2 will be answered in the following sections. First, Chapter 2 presents previous related research, the theoretical background of this research, and an overview related to 3D modeling techniques. This chapter provides a reference for the selection of parameters related to mangrove wave attenuation (sub-problem 1). The content includes the theoretical background of vegetation wave attenuation, and the relationship between some characteristic parameters of vegetation and wave attenuation. At the same time, it also includes related research on vegetation parameter measurement and application development and examples of using smart phones in the field of 3D scanning. Chapter 3 presents the basic methods and procedures for measuring mangrove parameters using the smartphone-based SfM-MVS. Chapter 4 focuses on experimentally determining the optimal conditions for the use of smartphone-based SfM-MVS methods, including photographic distance testing and light intensity testing (sub-problem 2). Chapter 5 presents the accuracy results and error analysis of the method for

measuring different mangrove parameters under the best conditions. Chapter 6 discusses the ability of the smartphone-based SfM-MVS method to reconstruct 3D models of mangroves based on the results of the previous chapters, focusing on the feasibility of this method for measuring mangrove parameters related to wave attenuation. Recommendations also be listed in Chapter 6. Finally, Chapter 7 makes conclusions for this research and answers the research questions in Section 1.2.

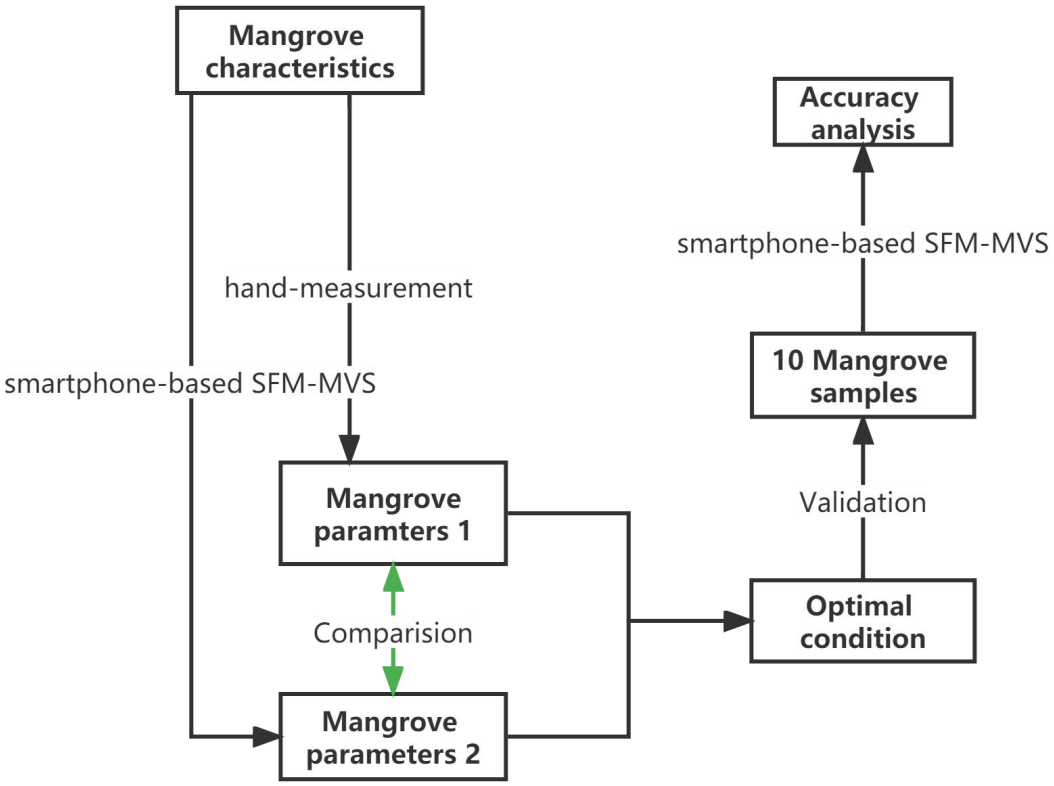

Figure 1.2: Schematic overview of the research approach

2. Literature review

2.1. Wave attenuation due to vegetation

Despite the complex geometric complexity of mangroves, numerical models often simplify vegetation by representing it as rigid cylinders (Suzuki et al., 2012). On this basis, several studies (eg, Dalrymple et al., 1984; Kobayashi et al., 1993) have represented vegetation in the form of cylindrical arrays and considered the force of waves on these structures. This cylindrical array approach relates some characteristics of vegetation (vegetation height, diameter and density) to wave attenuation, quantifying the direct relationship of wave attenuation to some vegetation parameters and wave conditions. (Tschirky et al., 2001)

In the earlier time, an equation was proposed by (Morison et al., 1950) for the axial force on a cylinder in an oscillating flow:

$$F_x = F_d + F_i = C_d u|u| + \frac{1}{2} C_m \frac{\pi}{KC} \frac{du}{dt} \quad (2.1)$$

From which：

$$F_x = \widetilde{F_x} / 0.5\, \rho\, U_{ref}^2 Ld \quad (2.2)$$

$\widetilde{F_x}$ is the dimensional flow force acting on the cylinder, ρ is the fluid density, U_{ref} is the reference velocity, L is the cylinder length, d is the cylinder diameter, u is the dimensionless flow velocity component（$u = u^{\sim}/U_{ref}$)，KC is Keulegan-Carpenter number（$= U_{ref}T/d$, T is wave period），t is the dimensionless time, C_m is the coefficient of inertia. Based on this, the drag coefficient of a cylinder in oscillating flow depends on two dimensionless parameters: namely KC (Keulegan-Carpenter number) and Reynolds number Re, where KC is related to the ratio of the oscillatory flow excursion length to the cylinder diameter, and Reynolds number $R_e = U_{ref}d/v$（v is the fluid kinematic viscosity）(Sarpkaya et al., 1981; Bouma et al., 2005).

The study by Etminan et al. (2019) modeled the emergent canopy as an array of rigid cylinders and used high-resolution numerical simulations to study the dynamics of oscillating flow through the emergent canopy. The impact of two mechanisms, the blocking effect and the shading effect, in changing canopy resistance was assessed. It was found that, at high KC, the blocking effect was the main mechanism responsible for the increase in the drag coefficient of the canopy in medium and high densities; while the shading effect played only a small role in reducing the drag coefficient of the very sparse canopy (Etminan et al., 2019).

The classical equation for wave attenuation was proposed by Dalrymple et al. (1984) and is applicable to medium and deep water wave conditions. In their formulas, H_t is the transmitted wave height , H_i is the wave height normalized by the incident wave, and they are a function of the transshore distance x of the vegetation through which the wave propagates, given by:

$$\frac{H_t}{H_i} = \frac{1}{1+\alpha x} \tag{2.3}$$

From which α is the wave height attenuation coefficient, expressed as:

$$\alpha = \frac{4\bar{A}_t N H_i C_D k}{9\pi} \frac{\sinh^3(kd)+3\sinh(kd)}{\sinh(kh)(\sinh(2kh)+2kh)} \tag{2.4}$$

$\bar{A}_t$ is the average projected area per unit height of each tree, N is the number of vegetation per unit area, h is the water depth, d is the average wet height of the vegetation, k is the wavenumber ($2\pi / L$), and L is the wavelength. Assuming that the random wave has a Rayleigh distribution, the peak wavenumber kp related to the peak period Tp is considered, and the root mean square wave heights $H_{rms,i}$ and $H_{rms,t}$ of the incident and transmitted waves are considered respectively. Finally, the wave attenuation coefficient $\tilde{\alpha}$ is given as:

$$\alpha = \frac{\bar{A}_t N H_{rms,i} C_D k_p}{3\sqrt{\pi}} \frac{\sinh^3(k_p d)+3\sinh(k_p d)}{\sinh(k_p h)(\sinh(2k_p h)+2k_p h)} \tag{2.5}$$

Equations (2.3) and (2.5) have been widely used in studies to model the attenuation of wave height by vegetation (Kelty et al., 2022).

Maza et al. (2019) conducted an experimental study of wave attenuation and drag along a 1:6 scale marginal mangrove mangrove with the aim of better understanding the physical processes behind parametric flow-mangrove interactions. It turns out that water depth, associated mangrove frontal area and wave height are the main variables driving the attenuation of shortwave waves (Maza et al., 2019). The study also used the wave attenuation equation extended by Mendez and Losada (2004), but here the damping coefficient was obtained after subtracting the additional friction from the bottom and side walls of the tank. Neglecting this additional damping will lead to an overestimation of mangrove wave dissipation capacity (Maza et al., 2019; Maza et al., 2021).

Other studies also reveal the correlation between vegetation parameters and wave attenuation. Zhang et al. (2021) investigated the wave-damping abilities of two contrasting dominant species in coastal salt marshes: the short, flexible Cyperaceae and the tall, stiff Poaceae. Parameters such as plant density, branch height, stem thickness, and seasonal changes in aboveground biomass were quantified in the two vegetation areas, respectively. The results suggest that aboveground biomass and height of swamp vegetation are key properties affecting the ability of vegetation to attenuate coastal waves (Zhang et al., 2021). Paul et al (2016) assessed the role of individual vegetation parameters in water-vegetation interactions. Stiffness, frontal area in still water, and material volume were manually controlled, and drag measurements were used as a reference. A comparison of several sets of experiments shows that stiffness and dynamic frontal area determine resistance. With constant stiffness and frontal area, force does not increase linearly with material volume (Paul et al., 2016). For vegetation densities, higher vegetation densities lead to smaller wave transmission coefficients and local wave heights (lou et al., 2018). After conducting wave dissipation experiments on willow forests, van Wesenbeeck et al. (2022) proposed that trees are

also hardly damaged under extreme wave conditions and strongly reduce the wave height. It was also observed that the surface area of the canopy was most correlated with wave attenuation, while the fragile leaves had a limited impact on wave attenuation.

2.2. Vegetation parameters measuring methods

The methods to characterize vegetation geometry can be divided into hand measurement and technical scanning methods. For hand measurement, the total frontal area of vegetation cannot be obtained directly by measurement tools, while it is a key parameter in wave attenuation related parameters. Strahler (1956) developed a bifurcated flow sequence scheme to understand and define river systems. McMahon and Kronauer (1976) proposed that the branching pattern of any tree species is self-similar, and any part of the tree can be used as a model for the whole tree. On the basis of their findings, Järvelä (2004) developed a method to determine the projected area of leafless trees, applying Strahler's (1956) stream sequence scheme to tree branching structures. This sorting method starts from the smallest branch of the tree and goes up to the trunk, and consists of 3 rules. First, the smallest branch is represented in order 1. Second, two branches 'm' in the same order form a branch of order ‘m+1’ at their junction. Third, if there are two branches of unequal order, the order of the branch formed at their junction is equal to the order of the higher-order branch of the two branches. In both research of Antonarakis et al (2009) and Kalloe et al. (2022), the tree branch ordering method developed by Järvelä (2004) was used to determine the frontal projected area of a tree in the leafless state.But Antonarakis et al (2009) and Järvelä (2004) considered the total frontal surface area of the trees, while Kalloe et al. (2022) included the distribution of the area over the height of the trees.

The measurement of vegetation parameters by means of 3D modelling has been used in a large number of studies (Indirabai et al., 2019; Heinzel and Huber, 2017; Holopainen et al., 2011; Novotny et al., 2021; Yin and Wang, 2019; Miller et al., 2015). Terrestrial Lidar can provide detailed, objective, three-dimensional precise indicators of tree structure (Indirabai et al., 2019). Indirabai et al. (2019) used a hierarchical minimum segmentation method, combined with a supervoxel clustering method, and multiple regression techniques to perform 3D reconstruction of a single tree. The results show that the obtained results have a strong correlation with the in situ measurement results of the instrument. The method successfully reconstructs a high-precision, specific tree model. Compared with other TLS-based tree modeling methods, such as Hough transforms to estimate diameter at breast height (DBH) (Heinzel and Huber, 2017), quantitative structuring modeling (Holopainen et al., 2011), this method can produce more accurate 3D model for individual tree, which demonstrates that multiple forest parameters can be estimated simultaneously using TLS.

Yin and Wang (2019) first investigated the possibility of individual tree detection and delineation (ITDD) using light detection and ranging (LiDAR) data collected by drones. The tree height (TH) and canopy diameter (CD) of each mangrove were measured, and the effect of canopy aggregation

density on mangrove ITDD was analyzed. The results showed that the estimates of TH and CD reached a realted high accuracy (RMSE 6.3%-14.3% for TH and 15.7%–27.5% for CD). The measurement accuracy is highest for orphan trees with the lowest clustering density. Novotny et al. (2021) comparatively analyzed aerial (ALS) and ground (TLS) laser scanning and field data collection methods to estimate tree height (TH), diameter at breast height (DBH), canopy base (CB), and canopy diameter (CD). The results show that TLS and ALS methods outperform each other in accuracy in measuring different tree parameters. But compared with the ALS method, the TSL method consumes more time. Field measurements have the highest time efficiency (Novotny et al., 2021).

In the study of Miller et al. (2015), the potential of multi-view stereo photogrammetry of structure from motion (SfM-MVS) using a low-cost handheld camera to accurately measure trees was tested. The results show that SfM-MVS is able to estimate both 2D and 3D metrics with an accuracy comparable to laser scanning (i.e. lidar). Factors such as the tree position relative to its surroundings, the background scene, and ambient lighting appear to affect the model's success. SfM-MVS offers a low-cost alternative to currently used remote sensing techniques, and since it does not require specialized equipment, it can be used by people with little expertise or training (Miller et al., 2015).

Some vegetation parameters can also be obtained by constructing geometric numerical models of trees. Kelvin et al. (2022) developed a geometric tree model of Avicennia marina vegetation based on the measured tree parameters. Based on the model, the distribution of the frontal surface area of the tree with the tree height was well represented. In the process of constructing the tree geometry model, the approximate relationship between branch diameter, branch length and branch order is illustrated. This study have shown that the contribution of tree roots and canopy to wave dissipation of vegetation cannot be ignored. And the contribution of smaller branches to frontal surface area is significant, considering only stems and large branches will greatly underestimate the value of frontal area.

2.3. Smartphone-based SfM-MVS related research

As mentioned in Chapter 1, for 3D scanning of vegetation, smartphone-based SfM-MVS method has lower cost and higher convenience than methods such as TLS and ALS. To confirm this, simple comparations of parameters between TLS/ALS methods and Smartphone-based SfM-MVS are depicted in figure 1.1 and table 1.1 (Data collected from the Internet).

Name	Size/mm	Weight/g	Cost/euros	Group equipment required	Lab/Field
RIEGL VZ-400 laser scanner (normal laser system)	180×180×308	9600	50000	Yes	Field
Artec Leo 3D Scanner (professional handheld TLS)	231×162×230	3000	20000	No	Both
DJI Mavic 3 Drone (non-professinal drone)	347×283×108	800	3000	Yes	Field
Smartphone (e.g.iPhone 12)	146×71×7	164	0-700	No	Both

Table 1.1. Comparation between TLS/ALS methods and Smartphone SfM-MVS method.

Figure 1.1. Upper left: TLS; upper right: ALS; lower left: hand-held TLS; lower right: iphone 12

Obviously, compared to professional scanners, drones and other equipment used in most 3D scanning nowadays, smartphones such as iPhone 12 have much lower cost and higher convenience. This means that, regardless of accuracy, smartphone-based 3D modeling methods have clear advantages. Based on this, some studies have used smartphone-based 3D scanning methods and tested the relative performance of the method in different fields.

With recent advances in photogrammetric processing methods and sensor technology, smartphones represent new opportunities for ubiquitous low-cost sensors with great potential for structure-from-motion (SfM) photogrammetry (Jaud et al., 2019). "Structure from Motion" (SfM) photogrammetry is a novel, low-cost, and easy-to-operate photogrammetry technique for acquiring

high-resolution data over a range. SfM methods are based on matching features in multiple overlapping, offset images while automatically solving camera pose and scene geometry (Westoby et al., 2012). There have been multiple studies testing the feasibility and relative performance of this approach (Westoby et al., 2012; Jaud et al., 2019; Luetzenburg et al., 2021; Gollob et al., 2021; Mokroš et al., 2021).

Before smartphones, the SfM approach first relied on consumer-level digital cameras. Taking a large collection of photos with a digital camera to create a high-resolution digital elevation model (DEM). To initially evaluate the technique, Westoby et al. (2012) compared SfM-derived DEMs to similar models obtained using terrestrial laser scanning. The results show that even for complex terrain, decimeter-level vertical accuracy can be achieved using SfM (Westoby et al., 2012). After this, Jaud et al. (2019) performed SfM reconstructions of coastal cliffs using three different smartphones (Galaxy S7, Lumia 930, and iPhone 8). A terrestrial laser scanner (TLS) was also applied to provide a reference dataset to evaluate the quality of SfM reconstructions. Finally, all tested smartphone models obtained satisfactory cliff face reconstructions (mean error < 5 cm). The study also pointed out that the fan-shaped capture mode is better than the linear capture mode, but requires that the distance from the device to the cliff face is sufficient to ensure good image overlap (Jaud et al., 2019).

In 2020, the iPad Pro 2020 and iPhone 12 Pro were born, with novel built-in LiDAR sensors. Luetzenburg et al. (2021) studied the basic performance of LiDAR sensors and tested them on coastal cliffs in Denmark. The results are compared with the best Structure-from-Motion Multi-View Stereo (SfM MVS) point cloud structure. LiDAR sensors create high-resolution models of objects with side lengths > 10 cm with an absolute accuracy of ± 1 cm. Coastal cliffs up to 130 × 15 × 10 m in size were 3D modeled using the sensor with an absolute accuracy of ± 10 cm. This result marks the Apple LiDAR device as a cost-effective alternative to established remote sensing technology, with potential applications in the wider natural sciences (Luetzenburg et al., 2021).

There are also studies applying smartphone-based 3D measurement to trees. A study by Gollob et al. (2021) tested the assistance of 3D scanning technology based on smartphone radar sensors in the field of forest inventory (tree counting and breast height diameter measurement). The study used the Apple iPad Pro to generate 3D point clouds and compared the results with the Personal Laser Scanning (PLS) method. Tree mapping using the iPad showed a detection rate of 97.3%, while PLS scans detected 99.5% of the trees. The root mean square error (RMSE) of the best DBH measurement obtained using the iPad was 3.13 cm and using the PLS was 1.59 cm. The data collection time using an iPad is about twice as long as PLS, but 2.5 times shorter than a manual forest inventory device. Thus, iPad-based forest inventories are generally feasible and enable accurate stem counts and dbh measurements compared to manual methods (Gollob et al., 2021). Mokroš et al. (2021) performed a similar experiment, using an iPad Pro 2020 and a handheld personal laser scan (PLS) to perform individual tree detection and breast height diameter measurements at the same site, respectively. Data provided by Terrestrial Laser Scanning (TLS) serves as a ground truth reference. The results were in agreement with the findings of Gollob et al. (2021) (rRMSE range of DBH was 3.7%-6.4%, and tree detection rate was 90.6%-100%).

Interestingly, when considering only trees with a DBH greater than 20 cm, the tree detection rate was 100% across all test sites. When the tree DBH threshold was changed from 7 cm to 10 cm and then to 20 cm, the accuracy of DBH measurements (rRMSE) and tree detection rates improved significantly for all devices (Mokroš et al., 2021).

3. Method

Based on literature studies, this chapter presents the basis of this study, the method for measuring mangrove parameters related to wave attenuation using smartphone-based structure from motion multi-view stereo-photogrammetry (SFM-MVS). First, Section 3.1 introduces the selection of mangrove samples, smartphone and 3D scanning application in this study. Based on the results of the literature review in Chapter 2, Section 3.2 details the selection of mangrove parameters related to wave attenuation. Section 3.3 illustrates how to use a smartphone for image acquisition and 3D model reconstruction of sample trees. And in Section 3.4, the method to measure the desired tree parameters from the reconstructed 3D model is presented. For comparison and verification, Section 3.5 introduces the method of actually manually measuring the true values of tree parameters. The last section 3.6 is the method of statistical analysis of the data.

3.1. Samples and Equipment

In this study, all mangrove samples were collected at the mangrove greenhouse of the Deltares Institute in the Netherlands (Figure 3.1). Among them, 2 samples were used to analyze the best conditions, and 10 samples were used to analyze the accuracy of the method. The greenhouse simulates the field growth conditions of mangroves in the tropical intertidal zone, such as soil, moisture, temperature, etc. Among them, several specimens of *Avicennia marina* with different ages/heights were selected for samples. The data collection period for the experiment was from May to August 2022. Due to the large span of data collection time, our manual measurement and mobile 3D scanning of the same mangrove individual were completed at the same time, thus avoiding experimental errors caused by the growth of mangroves.

The choice of equipment and software for the SFM-MVS of the mangrove samples was carefully considered. So far, the iPhone 12 pro is the first smartphone to feature a native LIDAR sensor, which enables it to capture 3D scenes directly in the field. The original purpose of developing iPhone LIDAR was to enhance the focusing ability of the phone (especially at low brightness), but the program developers developed its 3D capture ability, so several 3D scanning applications were born (such as Pix4DCatch, 3D Scanner App, EveryPoint, Polycam, etc.) (Tavani et al., 2022). But except for polycam, all other applications need to be used on mobile devices with LIDAR sensors (ie iPhone 12 pro and iPhone 13 pro). Polycam can not only use LIDAR sensor for 3D capture of scenes, but also automatically reconstructs 3D models using overlapping 2D digital image sets by taking pictures without LIDAR sensors (it can be used on any mobile device equipped with an IOS system). In the professional mode of Polycam, object detail settings and object mask settings can be used to deal with objects of different levels of complexity. The reconstructed 3D model can be then exported in a number of different formats. In this study, for the universality and lower cost of the method, we use the regular iPhone 12 mobile phone (without LIDAR sensor) and the 3D scanning application software ‘Polycam’ as the tools for 3D scanning and modeling. The

dimensions of the iPhone 12 is 146.7 x 71.5 x 7.4 mm and the camera configuration is 1170 x 2532 pixels.

For manual measurement, flexible tape measure combined with vernier caliper were use to measure the required parameters with different sizes and were accurate to 0.5mm.

Figure 3.1. The mangrove greenhouse at the Deltares Institute in the Netherlands

3.2. Selection of parameters

To better investigate the role of mangroves in coastal protection to avoid redundance, this study focused on testing the potential of smartphone-based SfM-MVS in measuring mangrove parameters related to wave attenuation. Combined with the results of the literature survey in Chapter 2, the mangrove parameters measured in this study include linear parameters and frontal area (FA) at a certain height . Among them, the linear parameters of mangroves include tree height (TH), canopy diameter (CD), stem diameter (SD) and two branch diameters (BD1 and BD2). Tree height (TH) is the vertical distance from the highest point of a mangrove individual to the lowest point where it touches the soil. Note that we do not consider roots here, only the mangrove portion above the soil. Canopy diameter (CD) represents the horizontal distance from the extreme left to the extreme right of the tree in one direction.

For the selection of stem diameter (SD) and branch diameter (BD), we used a branch structure ordering method which was already introduced in Section 2.2. This method is called ‘Strahlers ordering scheme’ and is simply described in Figure 3.2.

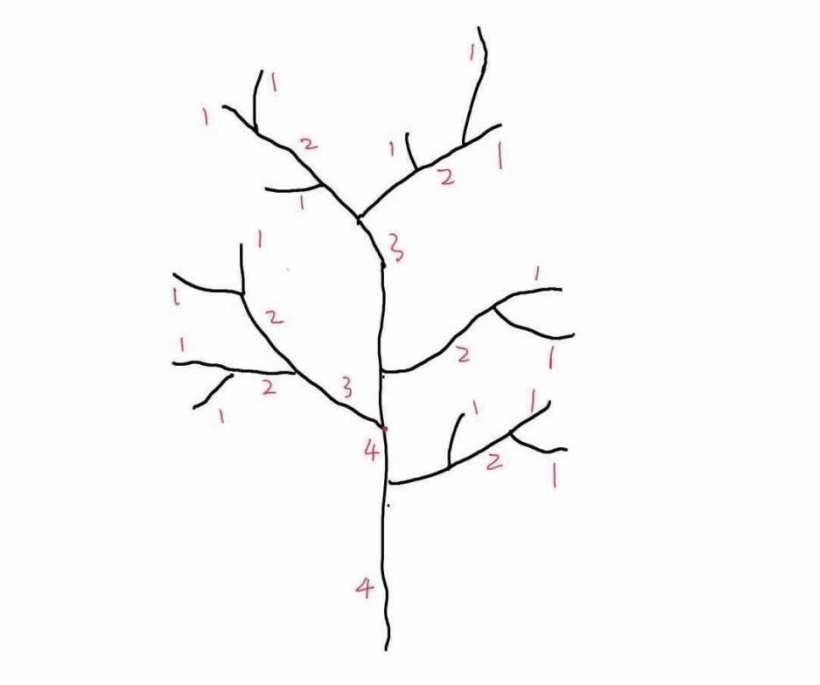

Figure 3.2. Strahlers ordering scheme

On this basis, SD represents the stem diameter of the highest order in the Strahlers ordering scheme (No. 4 in Figure 3.2). BD1 and BD2 represent the second and third higher-order branch diameters, respectively (No. 3 and 2 in Figure 3.2). So generally, for a tree individual, the order of size of the diameter is: SD>BD1>BD2. FA at a certain height is the sum of the diameters of the branches at a certain height. For each mangrove sample in this study, the frontal area was measured at four uniform heights (quintiles of tree height). All parameters can be visualized from Figure 3.3.

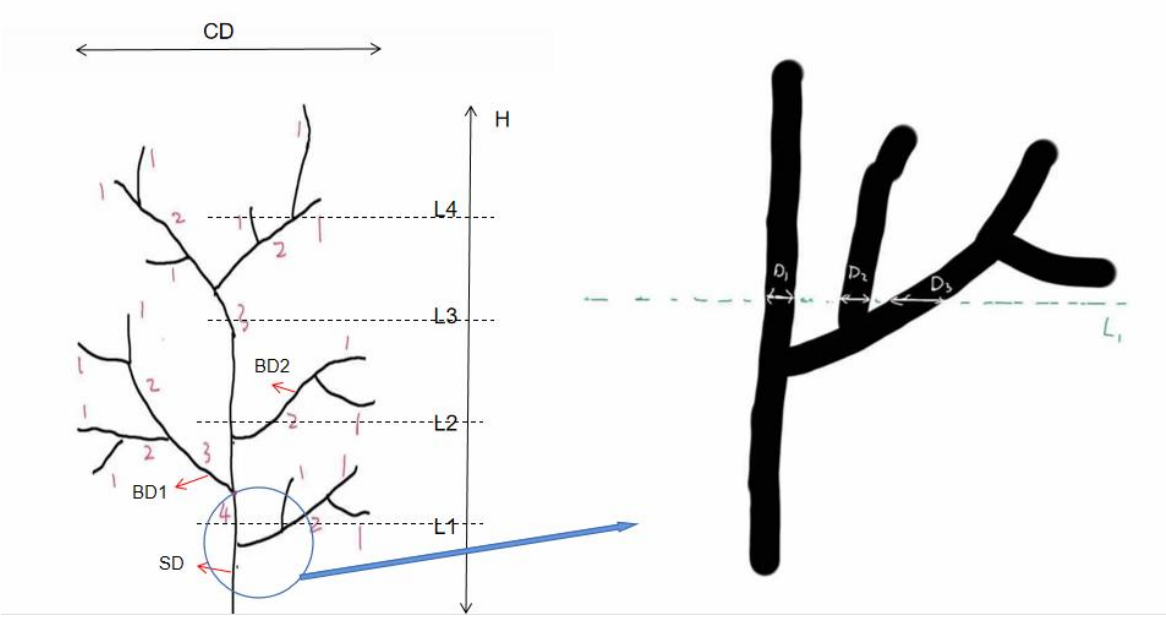

Figure 3.3. Parameter diagram (The right picture is an enlarged view of the yellow circled part of the left picture, where FA1=D1+D2+D3 at the height of L1).

It is worth noting that since each branch can be regarded as a cylinder with different diameters, in general, the horizontal diameter of the branch measured in any direction at a height is the same. An example is shown in Figure 3.4, where the red arrow represents the direction of wave propagation (x-axis direction), and the blue cylindrical section is the horizontal section of the branch at the height H to be measured. The frontal view and the side view of the wave direction are given in Figure 3.5, where d1 is the actual frontal area of the branch at this height that should be measured. Obviously, when the branch has a certain angle α relative to the wave propagation direction, the horizontal diameter of the branch measured from any direction is the same (d1=d2), so there is no error for the frontal area. But when the branch is almost parallel to the direction of wave propagation, that is, the α angle is very small, it may cause errors in our measurements. In this case, the measured value is d3, while the actual frontal area of the branch at this height is d1, and obviously d3>d1. In simple terms, measurement error occurs only when the direction of the branch is almost parallel to the direction of wave propagation. Generally, it can be assumed that waves propagate in a plane parallel to the ground. Therefore, when the direction of wave propagation is not assumed, only branches that are approximately parallel to the ground may experience measurement errors. Due to the phototropism of vegetation, branches generally tend to grow upwards (Yamamoto et al., 2002), so the above situation is extremely rare during the measurement process of this experiment. Thus, this potential error can be ignored in subsequent experiments.

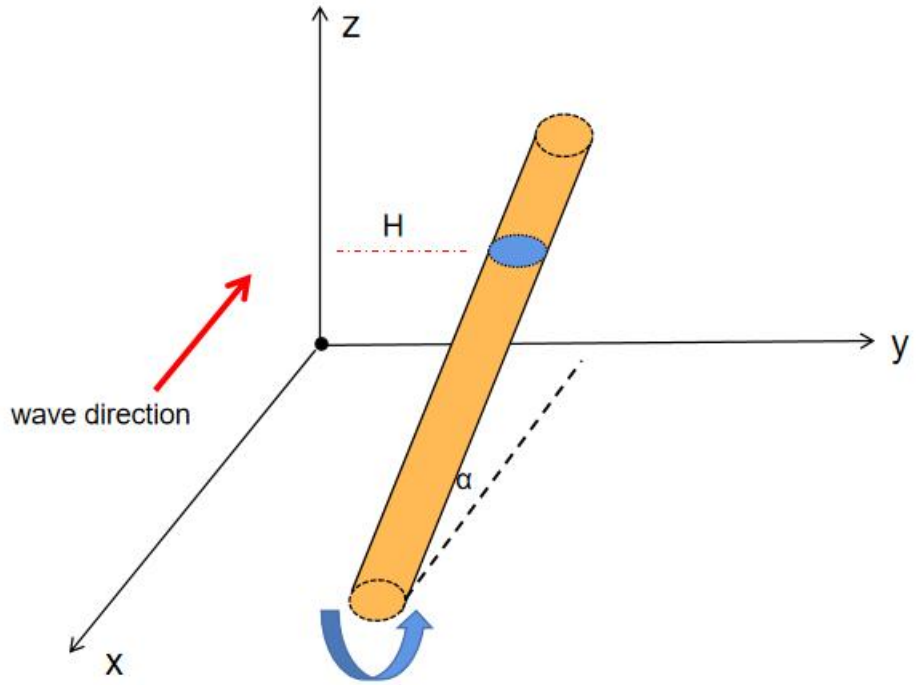

Figure 3.4. 3D branch schematic diagram. The red arrow is the wave propagation direction (the x-axis direction), and the blue section is the horizontal section of the branch to be measured at height H.

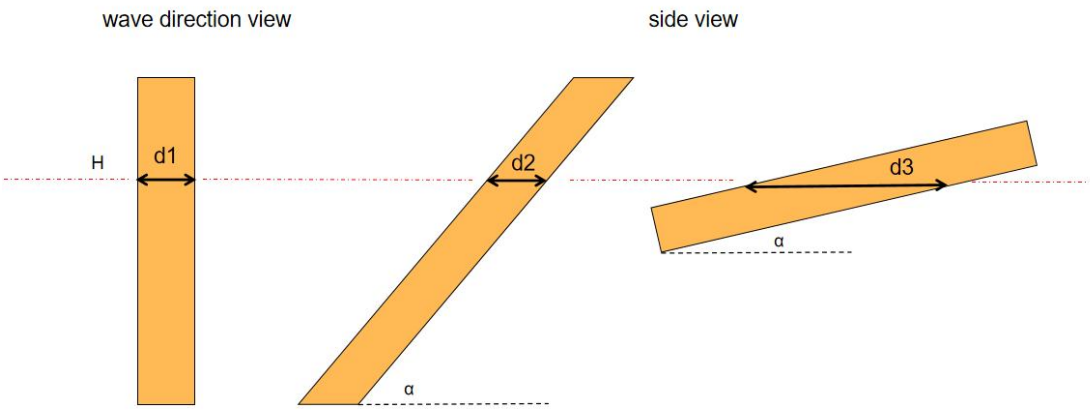

Figure 3.5. Front and side views of the branch in Figure 3.4 relative to wave direction. d1 is the frontal area of the branch at the height H that should be measured, and d2 and d3 are the actual measurements of the frontal area at different branch inclination angles. d1=d2, d3>d1.

3.3. 3D modeling using smartphone-based SfM-MVS

The mangrove samples were imaged using the automatic camera mode of the mobile phone app 'Polycam'. In this mode, the smartphone's position was slowly moved along a uniform concentric circular path. 'Polycam' automatically captures images of the sample in different orientations at regular intervals and ensures that there is at least 50% overlap between any two captured photos. Since the shape of the trees is irregular, the shape of each circular path is only an approximate circle. The 'Polycam' can only capture up to 250 photos at a time, so depending on the size of each mangrove sample, complete 3-5 circular paths from top to bottom (or bottom to top). Each circular path yielded 50-80 photos, and each mangrove sample yielded 250 photos. A brief schematic diagram is shown in Figure 3.4. During the image acquisition process, the distance between the phone and the tree is kept basically the same. The test of the most suitable photography distance and light condition is introduced in the next chapter.

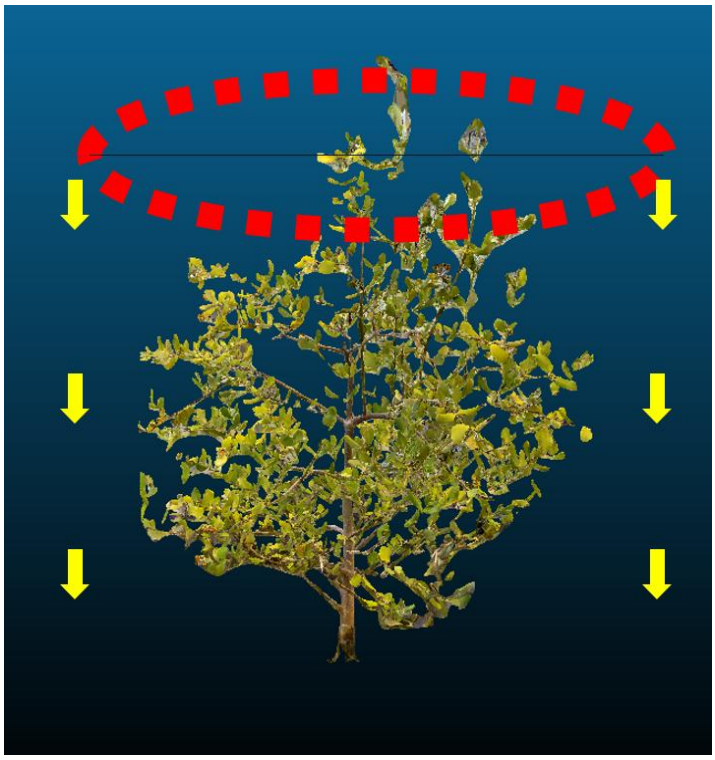

Figure 3.4. Image acquisition process. The red square can roughly represent the location of the smartphone.

After the image capture is complete, the model details are set to original and enable object masking mode. Then 'Polycam' can directly upload and analyze the collected 2D images and convert them into 3D models in less than half an hour in total. This means that both SfM(Structure-from-Motion) and MVS (Multi-View Stereo) processes were automatically completed in 'Polycam' in less than 10 minutes. Compared to normal SfM-MVS methods (e.g. Miller et al., 2015; Morgenroth and Gómez, 2014), this process is obviously greatly simplified.

Figure 3.5. Model generation stage： the left picture is the original tree, the right picture is the 3D model generated by Polycam.

3.4. Measurements in Cloudcompare

Linear measurements were performed on the 3D model to estimate tree height, canopy diameter, stem diameter, branch diameter and frontal area at a height of the mangrove samples. The mangrove 3D model generated by 'Polycam' was imported into the 3D point cloud analysis software 'Cloudcompare' in point cloud format (.ply). The rendering and cropping of 3D point clouds were completed in Coulcompare, some unwanted environmental impurities (such as adjacent trees, soil bases, etc.) were removed, and only the target mangrove individual was retained. To ensure that the target distance estimated from the 3D model is exactly the same linear distance as measured manually in the field, the measurement points are marked on the sample tree with brightly colored markers. This step is done before the capture, so the marker points are also visible in the 3D point cloud. Figure 3.6 shows an example of marked points on a sample tree. In the 'Cloudcompare' software, the distances at the marker points are measured to estimate the linear metrics of the sample tree. A schematic diagram of the measured parameters has been given in Figure 3.3.

For canopy diameter measurements, sometimes the markings at the end of the branch cannot be visualized in the 3D model, because the end of the branch cannot be modeled due to the slenderness of the end. In this case, the visible canopy diameter in the same direction as the marking is measured. The stem and branch diameters measured are their cross-sectional diameters at the mark. The frontal area at a height is obtained by adding the horizontal diameters of branches at a height. This means measuring the horizontal diameter of all branches at this height rather than the cross-sectional diameter of the branches themselves.

Figure 3.6. Example of marked points on sample trees: blue markers for measuring stem diameter and branch diameter; red markers for measuring frontal area at a certain height. (left figure is real tree measured by hand, right figure is SfM-MVS measured in Couldcompare)

3.5. Field hand-measurement for verification

Traditional hand-measurement was used in the field to validate the estimates of the parameters of the smartphone-based SfM-MVS model. A flexible tape measure was used to measure the vertical distance between the bottom of the sample tree (outside the soil) and the highest point of the branch, which is the tree height. The canopy diameter was measured by measuring the horizontal distance between the leftmost and rightmost branch ends (marked) in one direction. A vernier-caliper was used to measure the stem diameter and branch diameter at the marks on the main stem and branch. The vernier caliper was also used to measure the horizontal diameter of all branches at a marked height to obtain the frontal area at that height. All linear measurements are rounded to 0.5 mm accuracy.

3.6. Statistical Analysis

All data in this study were analyzed using Excel combined with Matlab. The accuracy of estimating mangrove parameters related to wave attenuation was assessed using error, absolute error(AE), root mean square error (RMSE) and bias. The following equations (1)(2)(3)(4) define these values.

$$\text{Error} = x_i - x_0 \quad (1)$$

$$\text{AE} = |x_i - x_0| \quad (2)$$

$$\text{RSME} = \sqrt{\frac{\sum_{i=1}^{n} (x_i - x_0)^2}{n}} \quad (3)$$

$$\text{Bias} = \frac{\sum_{i=1}^{n} (x_i - x_0)}{n} \quad (4)$$

where n is the estimated number of samples, x_i is the value estimated by the smartphone-based SfM-MVS, and x_0 is the hand-measured value.

On this basis, a linear regression analysis was also performed between the hand-measured true value and the SfM-MVS estimated value to obtain the R^2 value of the parameter values of the sample trees. This can make us feel the linear relationship between the two more intuitively.

4. The optimal usage conditions for smartphone-based SfM-MVS

Chapter 3 has already introduced methods for reconstructing mangrove models and measuring mangrove parameters using smartphone-based SfM-MVS. The following research will be based on this method to obtain the required data. Since this study is the first time to use a smartphone-based 3D modeling application (Polycam) to reconstruct the mangrove 3D model, it is necessary to test the optimal usage conditions of this method to better evaluate the measurement accuracy of this method. The first is the test of the photography distance of the mobile phone, which compares the errors of the parameters of the same mangrove sample obtained by three different photography distances, which is introduced in Section 4.1. This was followed by ambient light intensity testing, which included a resolution test, to identify light (weather) conditions suitable for reconstructing the mangrove model using the smartphone-based SfM-MVS method, as described in Section 4.2. In Section 4.3, another mangrove sample was used to verify this optimal condition.

4.1. Photography distance test

4.1.1. Photography distance test method

In the greenhouse, a moderately high mangrove individual was selected as the experimental sample. The tree is 3D modeled using the smartphone-based SfM-MVS method at photography distances of 10 cm, 25 cm, and 50 cm, keeping other conditions the same. For each image acquisition process, photography through more than three complete circular paths from top to bottom (or bottom to top) should be ensured. The schematic diagram is shown in Figure 4.1. Estimates of mangrove parameters were obtained in Couldcompare, and manual traditional measurements were used to verify errors.

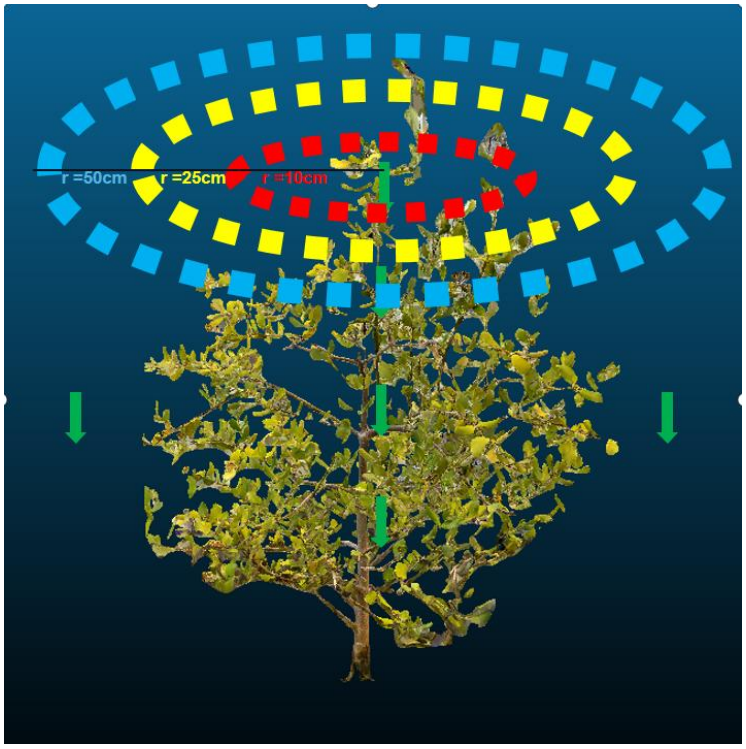

Figure 4.1. Smartphone-based SfM-MVS at different photography distances

4.1.2. Photography distance test results

In order to test the optimal photography distance of the smartphone-based SfM-MVS method, the errors of the smartphone-based SfM-MVS estimated data at three different photography distances are shown in Table 4.1. Figure 4.2 is for the convenience of intuitive comparison of the error of each parameter under the three photography distances. A negative sign indicates that the model underestimated the value of this parameter.

It can be see that for tree height, the measurement error at 25cm distance (-3.06%) is much smaller than that at 10cm distance (-15.42%) and 50cm distance (-13.96%), and the tree heights are all underestimated. For canopy diameter, the measurement error at 25cm photography distance is -3.21%, which is also better than other two photography distances (-6.33% and -7%, respectively), and canopy diameters are also underestimated. From the data results, the photography distance seems to have little effect on the measurement of stem diameter, and the error is less than or equal to 2%. But the photography distance of 25cm and 50cm makes the stem diameter slightly overestimated, and the photography distance of 10cm makes the stem diameter slightly underestimated. For thicker branch 1, it was slightly overestimated (4% error) at 10cm photography distance, slightly underestimated (-4%) at 25cm distance, and more underestimated at 50cm distance (-10.67 %). For the thinner branch 2, both 10cm and 25cm photography distances result in underestimated results (-14% and -12%, respectively), and at 50cm photography distance the branch was not even visible (error = -100%). For the frontal area at the

four heights, at the highest height, none of the three photography distances make branches at that height appear (error = -100%). For the other three lower heights, the errors obtained at the photography distance of 25cm are all smaller than those obtained at the distances of 10cm and 50cm, and the differences are between 5% and 15%. At all four heights, the frontal area is severely underestimated, with the smallest error of -66.67%. Combining the data comparison between the figure and the table, it is not difficult to see that the photography distance of 25cm is better.

Metric	Distance 10cm	Distance 25cm	Distance 50cm
Tree height	-15.42%	-3.06%	-13.96%
Canopy diameter	-6.33%	-3.21%	-7.00%
Stem diameter	-1.22%	2.04%	1.22%
Branch diameter 1(thicker)	4.00%	-4.00%	-10.67%
Branch diameter 2(thinner)	-14.00%	-12.00%	-100.00%
Frontal area at L1	-76.69%	-71.43%	-79.70%
Frontal area at L2	-70.00%	-66.67%	-72.22%
Frontal area at L3	-92.16%	-86.27%	-100.00%
Frontal area at L4	-100.00%	-100.00%	-100.00%

Table4.1. Error of parameters at different photography distances

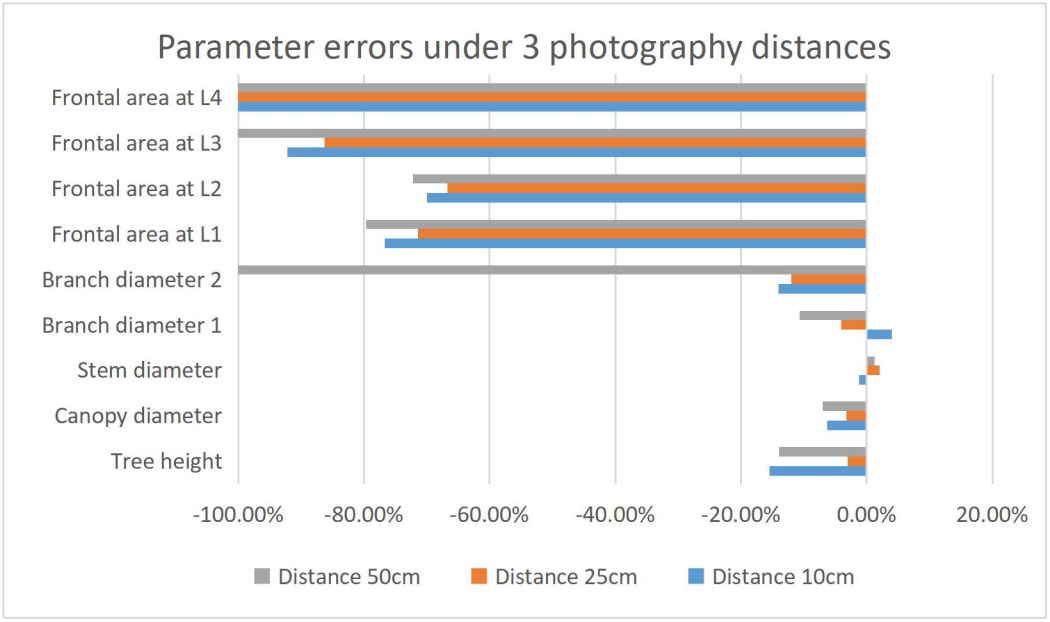

Figure 4.2. Comparison of parameters error under 3 photography distances

4.2. Ambient light intensity test

From the experimental results of the photography distance test, the performance of the smartphone-based method does not seem to be ideal, especially for the frontal area at a certain height, the error of the parameter estimation is large. This is due to the fact that the ambient light intensity is not considered. In the actual measurement work, the illumination of the environment will change with the weather, which may greatly affect the accuracy of the SfM-MVS method. Therefore, an ambient light test is also required to determine an optimal light condition (weather condition).

4.2.1. Method of ambient light intensity test

The same sample mangroves as used in the photography distance test were selected and smartphone-based SfM-MVS was performed on them under three weather conditions: sunny (light intensity around 9000 lux), cloudy with sunshine (light intensity around 4000 lux), and Cloudy with no sun (light intensity around 1000 lux). Based on the results of the photography distance test, the best photography distance of about 25cm is guaranteed during the image acquisition process. Ambient light intensity is determined by an Apple app called Lux Light Meter Pro.

4.2.2. Results of ambient light intensity test

The original data table of the parameters is shown in the appendix, and the error results of the parameters under different light intensities are shown in Table 4.2 and Figure 4.3. A negative sign indicates that the model underestimated the value of this parameter.

Metric	Sunny 9000 lux	Cloudy with sunlight 4000 lux	Cloudy without sunlight 1000 lux
Tree height	-5.76%	-2.43%	-1.32%
Canopy diameter	-8.10%	2.78%	3.38%
Stem diameter	-2.04%	-4.08%	-2.45%
Branch diameter 1(thicker)	-10.67%	-8.00%	-4.00%
Branch diameter 2(thinner)	-30.00%	-12.00%	-8.00%
Frontal area at L1	-78.20%	-65.41%	-54.14%
Frontal area at L2	-71.11%	-56.67%	-46.67%
Frontal area at L3	-92.16%	-84.31%	-72.55%
Frontal area at L4	-100.00%	-100.00%	-83.33%

Table 4.2. Error of parameters under 3 different weather & light intensity conditions.

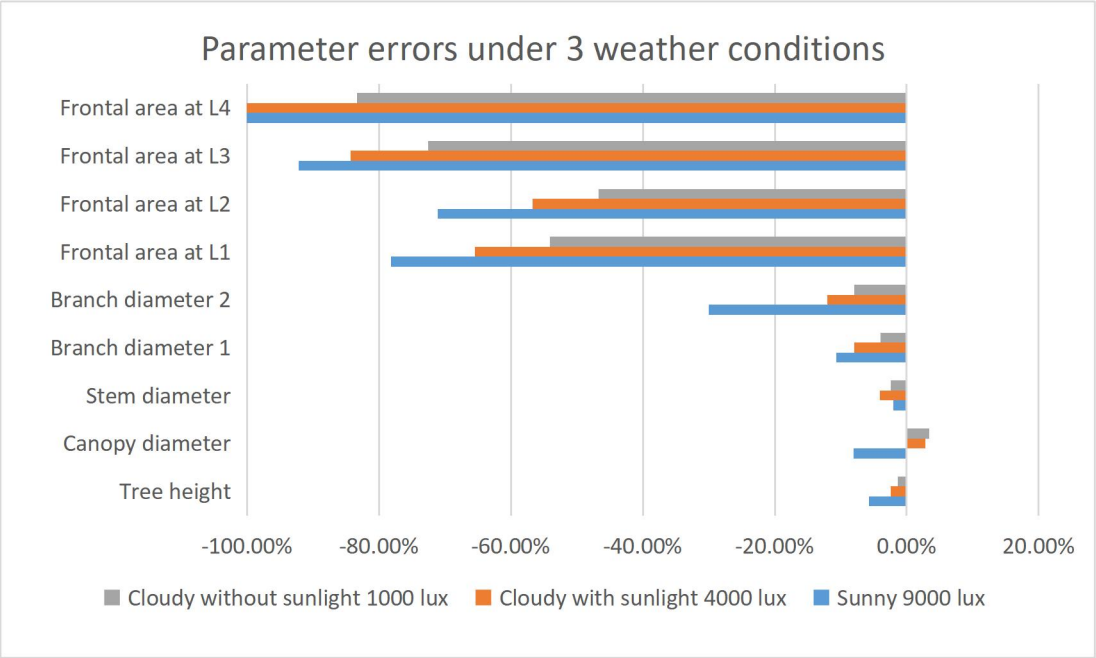

Figure 4.3. Comparison of parameters error under 3 different weather & light intensity conditions.

Figure 4.3 shows that for tree height, the measurement error at 1000 lux and 4000 lux (-1.32% and -2.43%, respectively) are smaller than that at 9000 lux (-5.76%), and the tree height is underestimated. For the canopy diameter, the 1000 lux and 4000 lux light conditions make the canopy diameter slightly overestimated, but the error is small (3.38% and 2.78%, respectively), while the 9000 lux light condition makes the canopy diameter underestimated, the error value is also larger (-8.1%). Similar to the results of the photography distance test, the light conditions don't seem to have a significant effect on the stem diameter measurement, and the error range is less than or equal to 4%, and all are slightly underestimated. For the thicker branch 1, it is slightly underestimated at 1000 lux (-4% error) and more underestimated at 4000 lux and 9000 lux (-8% and -10.67% error, respectively). For the thinner branch 2, the error increases significantly, the results under both 1000 lux and 4000 lux light conditions are underestimated (-8% and -12%, respectively), while at 9000 lux the result is severely underestimated: the error reaches -30%. For the frontal areas at four heights, the error obtained under the 1000 lux light intensity condition is the smallest, followed by the error obtained under the 4000 lux light intensity condition, and the largest error is obtained under the 9000 lux light intensity condition, the difference between adjacent two is about 10%. At all four heights, the frontal areas are still largely underestimated, but under cloudy without sunshine condition (light intensity of 1000 lux), the estimated error value of the frontal area at a certain height can already be reduced to less than 50%. Combining the data comparison between the figure and the table, it is obvious that the weather conditions are more suitable for cloudy days without sunshine.

4.2.3. Limit resolution test

4.2.3.1. Test setup

To test the limit resolution of the smartphone-based SfM-MVS method, the resolution of the method was tested under different light intensities. A simple platform was built for this, and 7 branches of different diameters were inserted side by side, with diameters of 17mm, 11cm, 8mm, 6mm, 5mm, 3mm and 2mm, as shown in Figure 4.4. Under outdoor conditions, the tree branch platform was captured and 3D modeled by Polycam at four moments of different light intensities on the same day. The measurement of light intensity is also done using 'Lux Light Meter Pro', the unit of light intensity is lux.

Figure 4.4. Simple platform with 7 branches of different diameters

4.2.3.2. Test result

At the moment when the light intensity is 10000 lux, 1500 lux, 300 lux and 60 lux, respectively, the 3D model of the branch platform is reconstructed using the smartphone-based SfM-MVS, and the visualization degree of the obtained 3D model is shown in Figure 4.5. At 10000 lux, the model only includes a small selection of branches with diameters of 17mm, 11mm and 8mm. Under the light intensity of 1500 lux, the 3D model can see branches with diameters of 17mm and 11mm, and some branches with diameters of 8mm and 6mm. At a light intensity of 300 lux, branches with diameters of 17 mm, 11 mm, 8 mm and 6 mm are visible, but only a small part of the branches of 5 mm and 3 mm are visible. Finally, under a light intensity of 60 lux, the model can display branches with diameters of 17mm, 11mm and 8mm and parts of branches with a diameter of 6mm, other branches are not shown.

(a) under 10000 lux

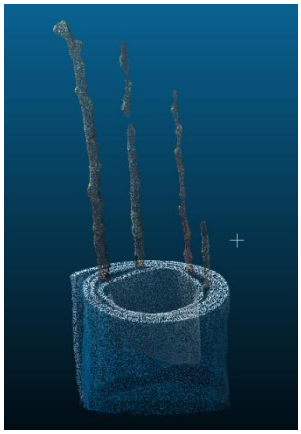

(b) under 1500 lux

(c) under 300 lux

(d) under 60 lux

Figure 4.5. Comparison of tree branch modeling resolutions under different light intensities

4.3. Validation of optimal usage conditions

From the results of the previous photography distance test and ambient light condition test, the photography distance of 25cm and the weather conditions on cloudy days without sunlight are the best conditions for smartphone-based SfM-MVS. To verify this condition, smartphone-based SfM-MVS was performed on a different mangrove sample (called tree 2) at a photography distance of 25cm and a cloudy and no sunlight environment. The error results for the parameters are compared to the results for the sample tree used in the best condition test (called tree 1). See Table 4.3.

Metric	Error of tree 1	Error of tree 2
Tree height(mm)	-1.32%	-9.77%
Canopy diameter(mm)	3.38%	-14.07%
Stem diameter(mm)	-2.45%	2.04%
Branch diameter 1(thicker)(mm)	-4.00%	-5.24%
Branch diameter 2(thinner)(mm)	-8.00%	-8.89%
Frontal area at L1(mm)	-54.14%	-5.81%
Frontal area at L2(mm)	-46.67%	-22.64%
Frontal area at L3(mm)	-72.55%	-37.50%
Frontal area at L4(mm)	-83.33%	-61.90%

Table 4.3. Comparison of parameter errors between tree 1 and tree 2. Tree 1 is the tree used in the best condition test before, tree 2 is another tree used for validation.

From the results, it can be seen that for tree 2 (for validation) , the model underestimates the tree height and canopy diameter, with errors of -9.77% and -14.07%, respectively. The error increased relative to the previously tested mangrove sample. The model slightly overestimated stem diameter by 2.04%. For two different classes of branches, the model underestimated their values (errors of -5.24% and -8.89%, respectively). Similar to the previously tested mangrove samples, the error was greater for thinner branches. Notably, for the validated mangrove sample, the accuracy of the model's estimated frontal area at a certain height improved. The error at the first height is even only -5.81%, the error of the frontal area at the second and third heights also drops below 40%, and the highest height still has the largest error value (-61.9%).

4.4. Conclusions

The purpose of this chapter is to determine the optimal conditions for the use of a smartphone-based SfM-MVS method for mangroves, and to lay the groundwork for subsequent determination of the method's performance in measuring mangrove parameters related to wave attenuation. First, the performance at three different photography distances was tested. According to the data results, it is obvious that the photography distance of 25cm is the best among them. But even at the photography distance of 25cm, the error of the parameters estimated by the model is still large, especially for the frontal area at a certain height. Moderate weather conditions and ambient light levels may be helpful for the accuracy. An ambient light intensity test was then performed to test the performance of the method in three weathers (three light intensities). According to the data analysis, the conditions of cloudy days and no light are the most suitable, and the obtained parameters have the smallest error. As expected, improving the lighting conditions did improve the accuracy of the model. From the experiment at the limit resolution, it can be concluded that as the light intensity decreases, the quality of the 3D model first increases and then decreases. In this test, the condition of 300lux is the best. The best time to scan outdoors is when it is cloudy (approximately 100-1000 lux of light). It is not suitable to use this SfM-MVS method outdoors on sunny days (light intensities typically greater than 5000 lux). This is

consistent with the results of the light intensity test. But even under suitable light intensity, branches with a diameter of less than or equal to 5mm cannot be accurately displayed, especially branches less than or equal to 3mm in diameter can hardly be seen. This indicates that the smartphone-based SfM-MVS method has limited modeling ability for smaller diameter branches (<=5mm).

5. Accuracy of smartphone-based SfM-MVS

The accuracy to be studied here refers to the accuracy when smartphone-based SfM-MVS is applied to measure mangrove parameters related to wave attenuation. The results in this chapter are based on SfM-MVS 3D model reconstructions of 10 mangrove samples of different ages and sizes. The mean, RMSE, and bias of field hand measurements and smartphone-based SfM-MVS estimates are shown in Table 5.1.

Metric	Mean (hand measured)	Mean (SfM-MVS measured)	RMSE(%)	Bias(%)
Tree height (mm)	1787	1595.4	13.51	-10.72
Canopy diameter (mm)	1314.5	1200	11.28	-8.71
Stem diameter (mm)	38.25	39.06	5.38	2.12
Branch diameter 1 (thicker) (mm)	22.3	22.3	4.78	0.00
Branch diameter 2 (thinner) (mm)	10.8	10.64	7.41	-1.48
Frontal area at L1 (mm)	110.9	77.35	36.35	-30.25
Frontal area at L2 (mm)	80.2	50.9	41.47	-36.53
Frontal area at L3 (mm)	73.15	43	46.41	-41.22
Frontal area at L4 (mm)	39.4	14.5	76.39	-63.20
Frontal area at a certain height (mm)	75.9125	46.4375	45.58	-38.83

Table 5.1. Comparison of hand measured and SfM-MVS measured values of mangrove parameters. The mean values, the root mean square error (RMSE) and bias of the model values are presented together.

5.1. Tree height and canopy diameter

From the results, the RMSE of estimated tree height is 24.14 cm (13.51%) with a bias of -19.16 cm (-10.72%). The bias is negative, indicating that smartphone-based SfM-MVS has a tendency to underestimate tree height. The linear regression results in Figure 5.1 show that although the smartphone-based SfM-MVS underestimates tree height to a certain extent, there is a strong linear relationship between the estimated height value and the hand-measured true value (R^2 = 0.9597) . The smartphone-based SfM-MVS estimates the canopy diameter with a good accuracy, with an RMSE of 14.83 cm (11.28%) with a bias of -11.45 cm (-8.71%), which also underestimates the canopy diameter to some extent. Regression analysis of canopy diameter estimates showed a strong correlation between estimated and measured values (R^2 = 0.8533, Figure 5.2).

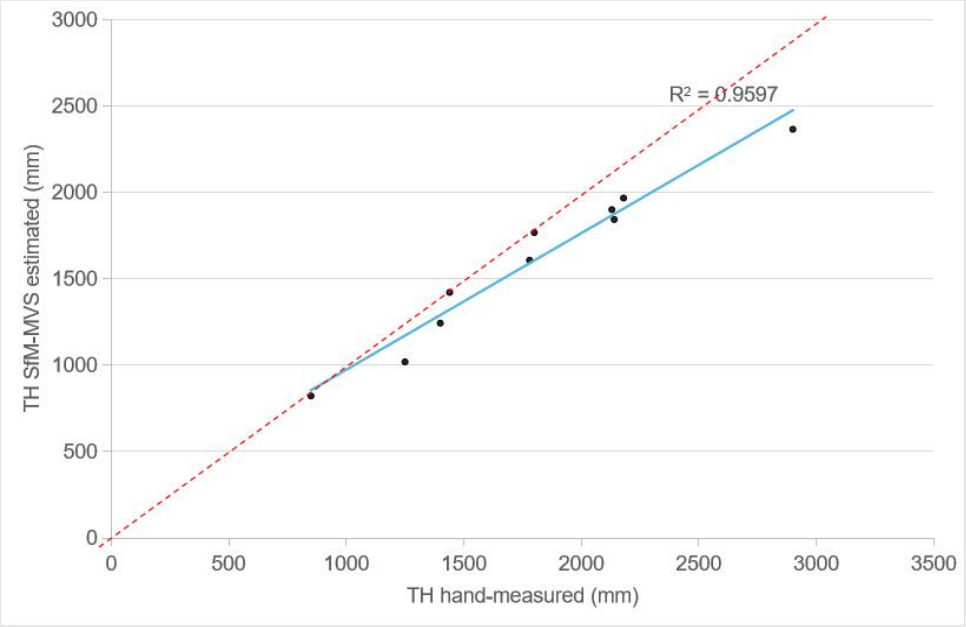

Figure 5.1. Regression analysis between smartphone-based SfM-MVS estimates and hand-measured true values of tree height (R^2 = 0.9597). The red dotted line with slope of 1, representing the case where the error is 0.

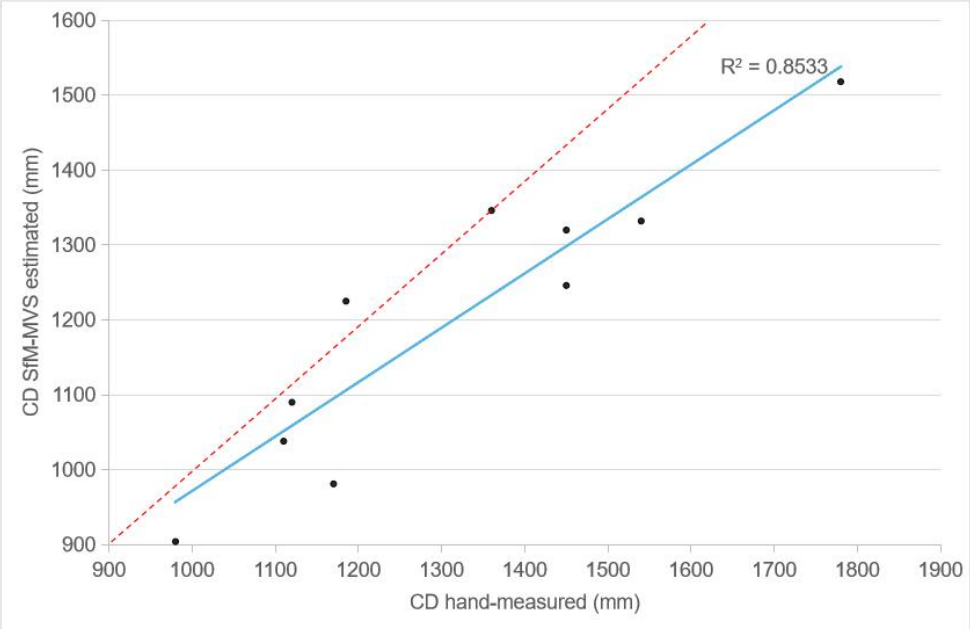

Figure 5.2. Regression analysis between smartphone-based SfM-MVS estimates and hand-measured true values of canopy diameter (R^2 = 0.8533). The red dotted line with slope of 1, representing the case where the error is 0.

5.2. Stem and branch diameter

The mean values of the hand-measured stem diameter and the estimated stem diameter from the SfM-MVS model were 38.25mm and 39.06 mm, respectively. Stem diameter was estimated with an RMSE of 2.06 mm (5.38%) and a bias of 0.81 mm (2.12%). The relationship of the linear regression in Figure 5.3 shows that the estimated value is highly correlated with the true value (R^2 = 0.9871). A bias of 2.12% indicates that the smartphone-based SfM-MVS slightly overestimates the stem diameter. The accuracy of estimating branch diameters with this method was similar to stem diameters. The estimated RMSE for the diameter of branch 1 was 1.07 mm (4.78%) with a bias of 0 mm (0%). A bias of 0 indicates that the smartphone-based SfM-MVS estimates the diameter of branch 1 very accurately, and generally does not tend to overestimate or underestimate. The accuracy of the estimate of the diameter of the thinner branch 2 decreased, with an RMSE of 0.8 mm (7.41%) and a bias of -0.16 mm (-1.48%). The negative bias indicates a tendency to slightly underestimate the diameter of branch 2 by smartphone-based SfM-MVS estimates. Meanwhile, the linear regression results in Figures 5.4 and 5.5 show that the smartphone-based SfM-MVS estimates of the diameters of two branches are highly correlated with the true values ($R^2$of 0.9921 and 0.9643, respectively).

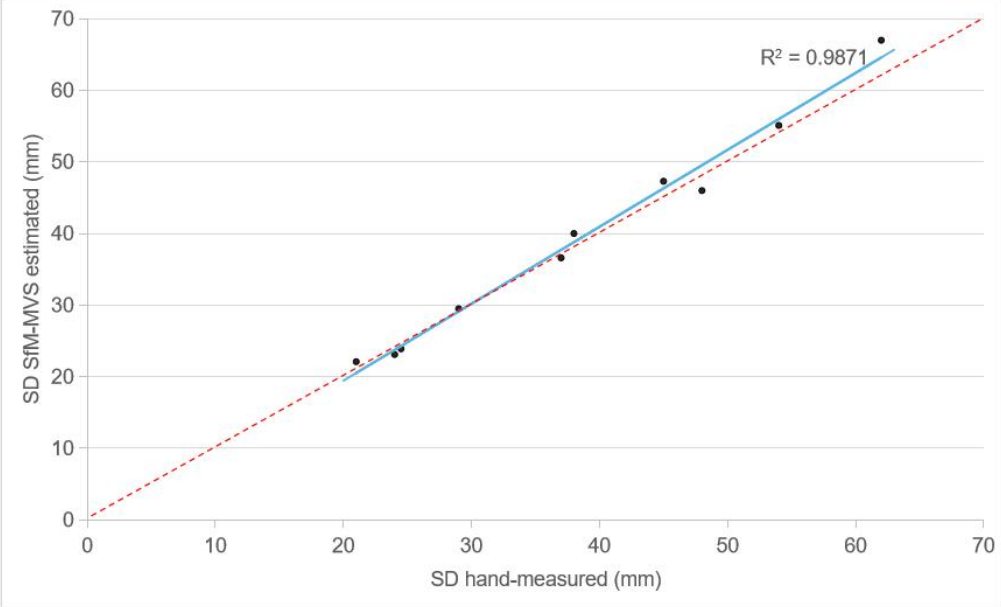

Figure 5.3. Regression analysis between smartphone-based SfM-MVS estimates and hand-measured true values of stem diameter (R^2 = 0.9871). The red dotted line with slope of 1, representing the case where the error is 0.

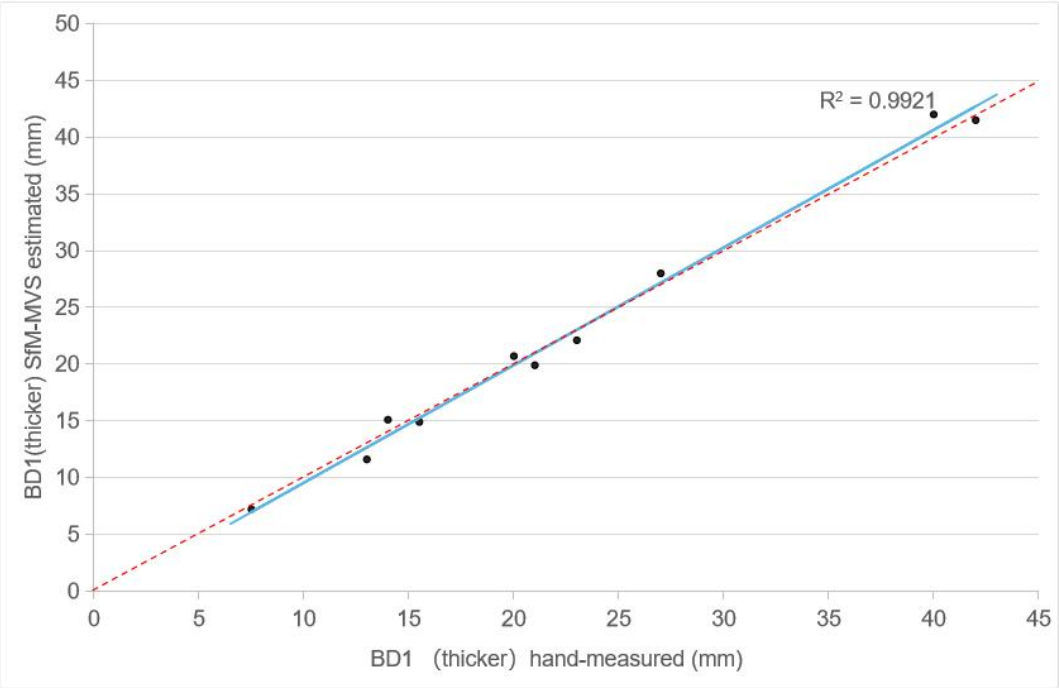

Figure 5.4. Regression analysis between smartphone-based SfM-MVS estimates and hand-measured true values of branch diameter 1 (R^2 = 0.9921). The red dotted line with slope of 1, representing the case where the error is 0.

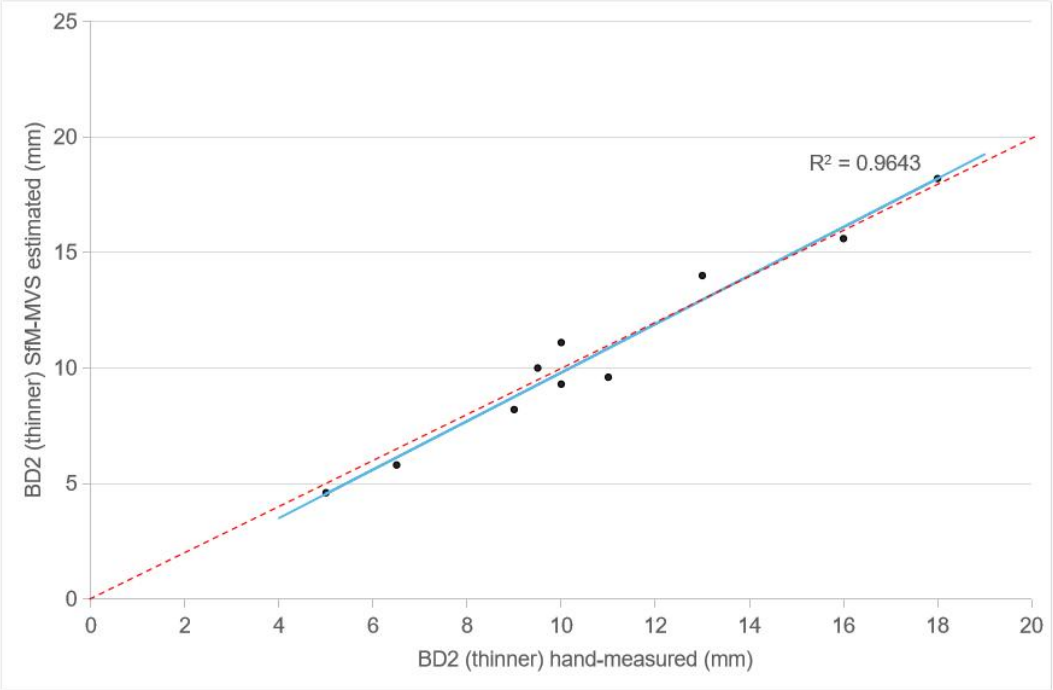

Figure 5.5. Regression analysis between smartphone-based SfM-MVS estimates and hand-measured true values of branch diameter 2 (R^2 = 0.9643). The red dotted line with slope of 1, representing the case where the error is 0.

5.3. Frontal area at a height

5.3.1. Accuracy

For each individual mangrove sample, we estimated the value of mangrove frontal area at four uniform heights (denoted as L1, L2, L3, and L4 from low to high, respectively). At height L1, the mean measured and mean estimated frontal area was 110.9 mm and 77.35 mm, respectively. The RMSE value was 40.31mm (36.35%), with a bias of -33.55mm (-30.25%); at height L2, the mean measured and mean estimated frontal area was 80.2 mm and 50.9 mm, respectively. The RMSE value was 33.26mm (41.47%), with a bias of -29.3mm (-36.53%); at height L3, the mean measured and mean estimated frontal area was 73.15mm and 43mm, respectively. The RMSE value was 33.95mm (46.41%), with a bias of -30.15mm (-41.22%); at height L4, the mean measured and mean estimated frontal area was 73.15mm and 43mm, respectively. The RMSE value was 30.1mm (76.39%), and the bias was -24.9mm (-63.2%). From the estimated results of the frontal area at four different heights, as the height increases, the frontal area decreases, and the RMSE of the estimated frontal area increases (from 36.35% at L1 to 76.39% at L4). The RMSE values are large and the biass are all negative, indicating that smartphone-based SfM-MVS tends to underestimate the frontal area at all four heights.

The estimates of the frontal area at the four heights are combined as the frontal area at one of the heights. The measured mean and the model estimated mean were 75.91 and 46.44 mm, respectively. The RMSE value estimated by the model was 34.6mm (45.58%), and the bias was -29.48mm (-38.83%). A linear regression analysis was performed between the total 40 frontal areas at the four heights estimated by the SfM-MVS model and the corresponding true values (Fig. 5.6), and the results showed a close correlation (R^2=0.8784).

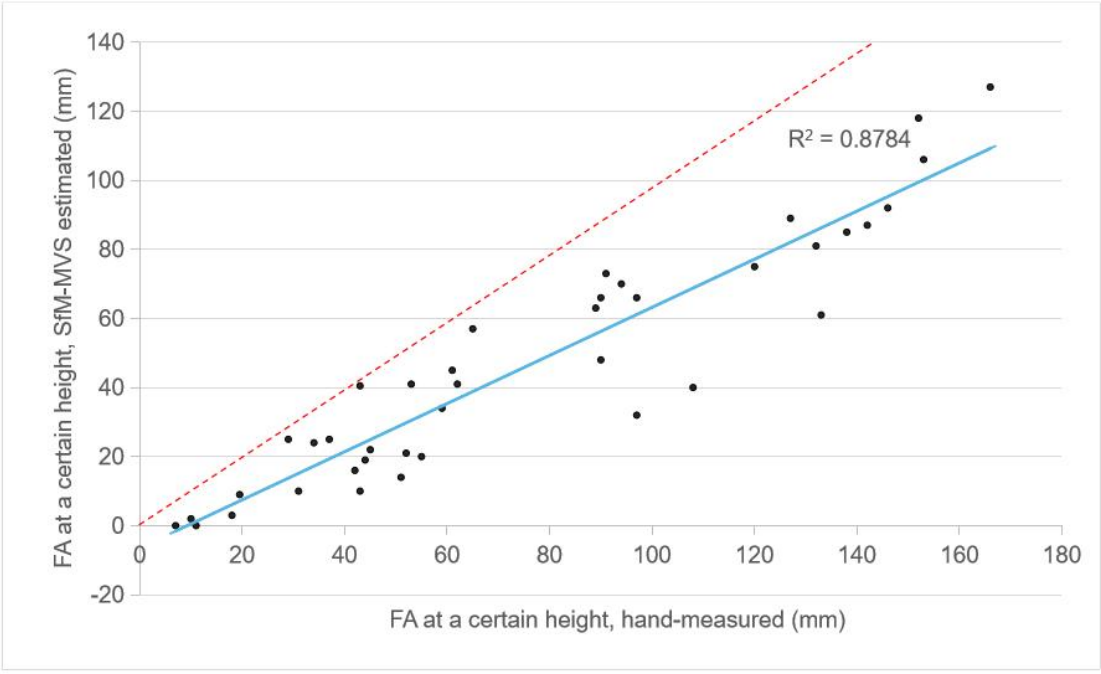

Figure 5.6. Regression analysis between smartphone-based SfM-MVS estimates and hand-measured true values of frontal area at a certain height (R^2 = 0.8784). The red dotted line with slope of 1, representing the case where the error is 0.

5.3.2. Influence of branch diameter and order

We consider that the relatively large RMSE of the estimated frontal area at a certain height is the reason for the weaker ability of smartphone-based SfM-MVS to model branches with smaller diameters. Based on the results of the resolution test in Chapter 4, we calculated the proportion of frontal area occupied by branches with a diameter of 5 mm or less at a certain height. And established a linear regression relationship between it and the error value (ie absolute error) of the frontal area at this height estimated by SfM-MVS, as shown in Figure 5.7. It can be seen that there is a strong correlation between them (R^2=0.8144).

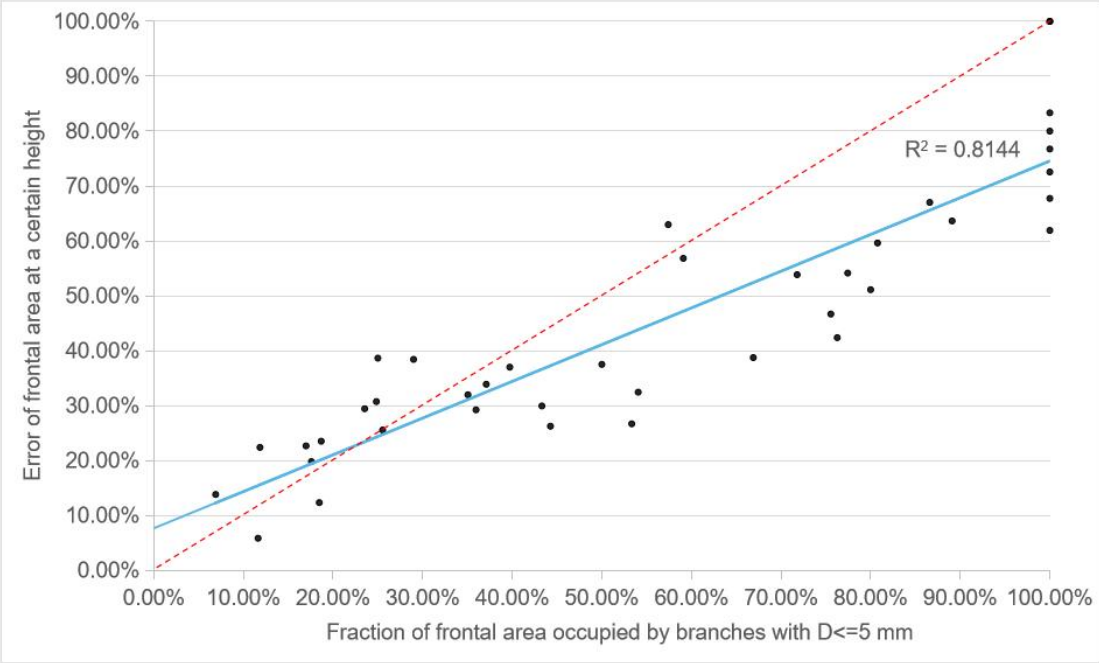

Figure 5.7. Regression analysis between the error of frontal area at a height estimated by smartphone-based SfM-MVS and propotion of frontal area occupied by branches with a diameter <= 5 mm at this height (R^2 = 0.8144). The red dotted line with slope of 1, representing the case of totally related.

The study done by Jerez Nova (2022) described the approximate relationship between branch order and diameter of mangrove individuals in different ages and densities. Based on this study, the 10 mangrove samples were divided into three categories: young trees, old sparse trees, and old dense trees. The approximate relationship between their branch orders and diameter ranges is shown in Table 5.2. Based on the measurements of branch diameters at each height and this table, the frontal area occupied by each order of branches at each height can be obtained. See appendix for tables of frontal area occupied by branches of each order at various heights for the 10 trees under hand measurement and smartphone-based SfM-MVS measurement. In this study, the

variable FA/SD was used to determine the effect of branch order on the measurement accuracy of the frontal area at a certain height. FA is the frontal area at a certain height and SD is the stem diameter. The purpose of this is to eliminate the effect of tree size as much as possible and to average the data for different type of trees so that the results are generalizable. Figure 5.8, 5.9 and 5.10 show: for young trees, old sparse trees and old dense trees, under the cases where all orders of branches are considered, the order 1 branch is ignored, and the order 1 and 2 branches are ignored, the gap between FA/SD value estimated by smartphone-based SfM-MVS and the true value measured by the hand at various heights.

Tree type \ Branch order	Order 1	Order 2	Order 3	Order 4	Order 5	Order 6
Young tree	1.5mm< D <=3mm	3mm< D <=5mm	5mm< D <=9mm	9mm< D <=25mm		
Old sparse tree	1.5mm< D <=4mm	4mm< D <=7mm	7mm< D <=13mm	13mm< D <=25mm	25mm< D <=55mm	
Old dense tree	1.5mm< D <=4mm	4mm< D <=7mm	7mm< D <=10mm	10mm< D <=14mm	14mm< D <=25mm	25mm< D <=55mm

Table 5.2. Relationship between branch orders and diameter ranges for different tree types

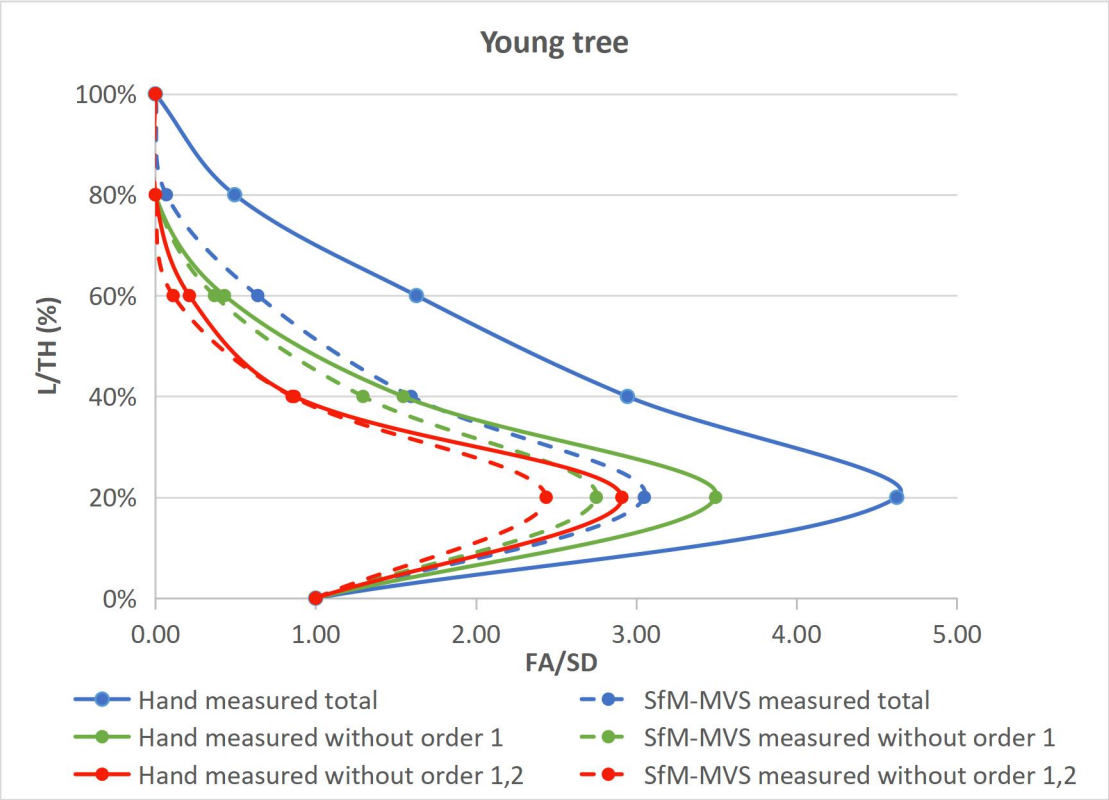

Figure 5.8. Gap of FA/SD between values estimated by smartphone-based SfM-MVS and the true values measured by the hand at various heights under different cases for young trees. Y-axis (L/TH) means measured height divided by tree height, 0%-100% means from bottom to top for a tree.

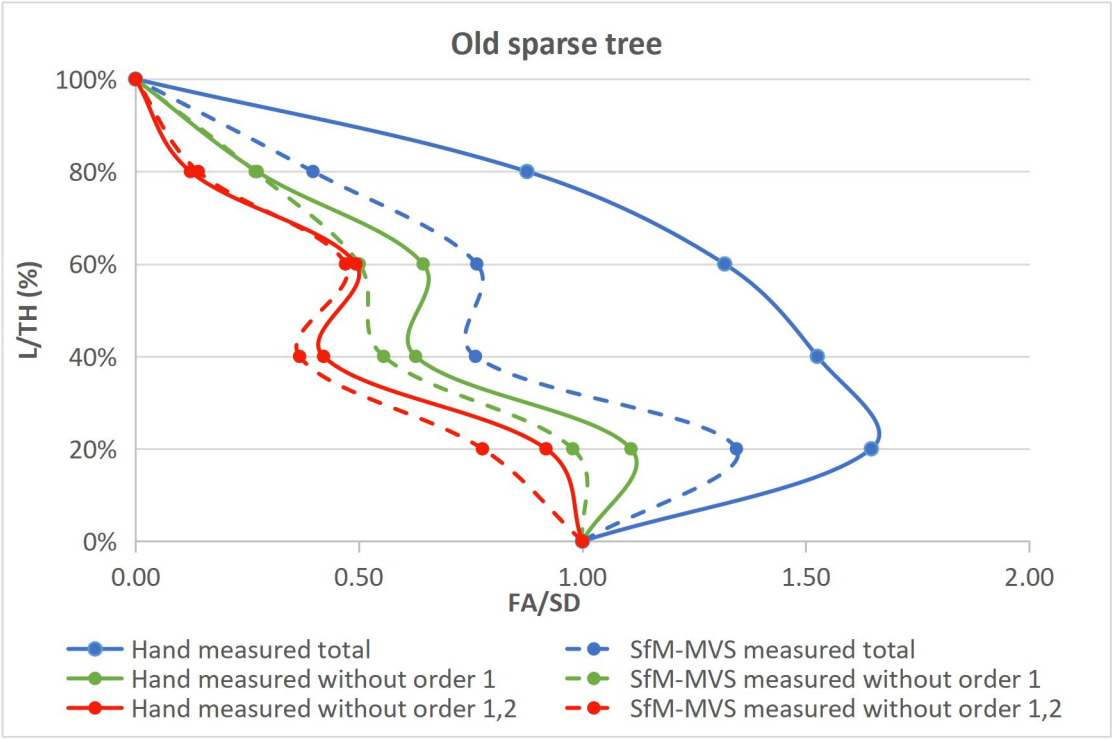

Figure 5.9. Gap of FA/SD between values estimated by smartphone-based SfM-MVS and the true values measured by the hand at various heights under different cases for old sparse trees. Y-axis (L/TH) means measured height divided by tree height, 0%-100% means from bottom to top for a tree.

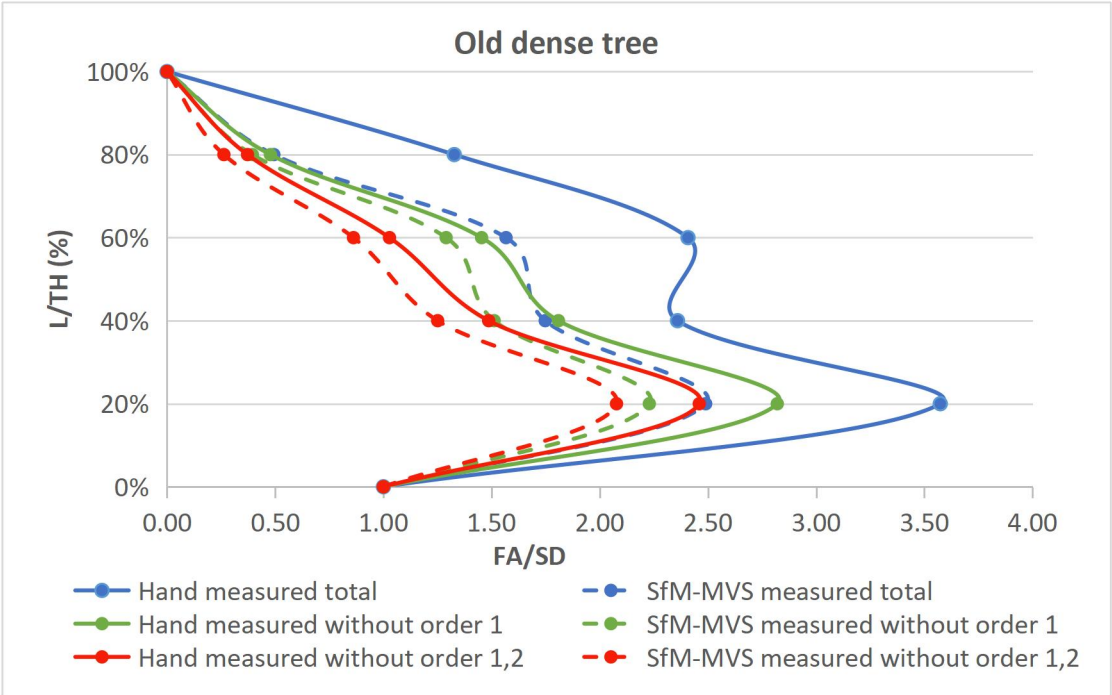

Figure 5.10. Gap of FA/SD between values estimated by smartphone-based SfM-MVS and the true values measured by the hand at various heights under different cases for old dense trees. Y-axis (L/TH) means measured height divided by tree height, 0%-100% means from bottom to top for a tree.

The distance between the solid blue line and the dashed blue line in Figure 5.8, 5.9 and 5.10 can represent the error of the total FA/SD value estimated by smartphone-based SfM-MVS at each height. The distance between the green solid line and the green dashed line represents the error of FA/SD value estimated by smartphone-based SfM-MVS at each height when the 1st order branches (i.e., the most terminal branches) are not considered. And the distance between the red solid line and the red dashed line represents the error of the FA/SD value estimated by smartphone-based SfM-MVS at each height when the 1st and 2nd order branches are not considered. From the omparasion of these 3 figures, the values of FA/SD for old sparse trees are relatively smaller. This may due to the less branches and so that less propotion of branches at a certain height for old sparse trees. In addition, the three figures have a remarkable common point: at each height, the distance between the solid blue line and the dashed blue line is much greater than the distance between the solid and dashed green and red lines. The distance between the green solid line and the green dotted line is not much different from the distance between the red solid line and the red dotted line. In other words, the estimation error of FA/SD is greatly reduced after ignoring branches of 1st order. Branch orders above order 2 no longer have a large effect on the accuracy of the FA/SD estimates.

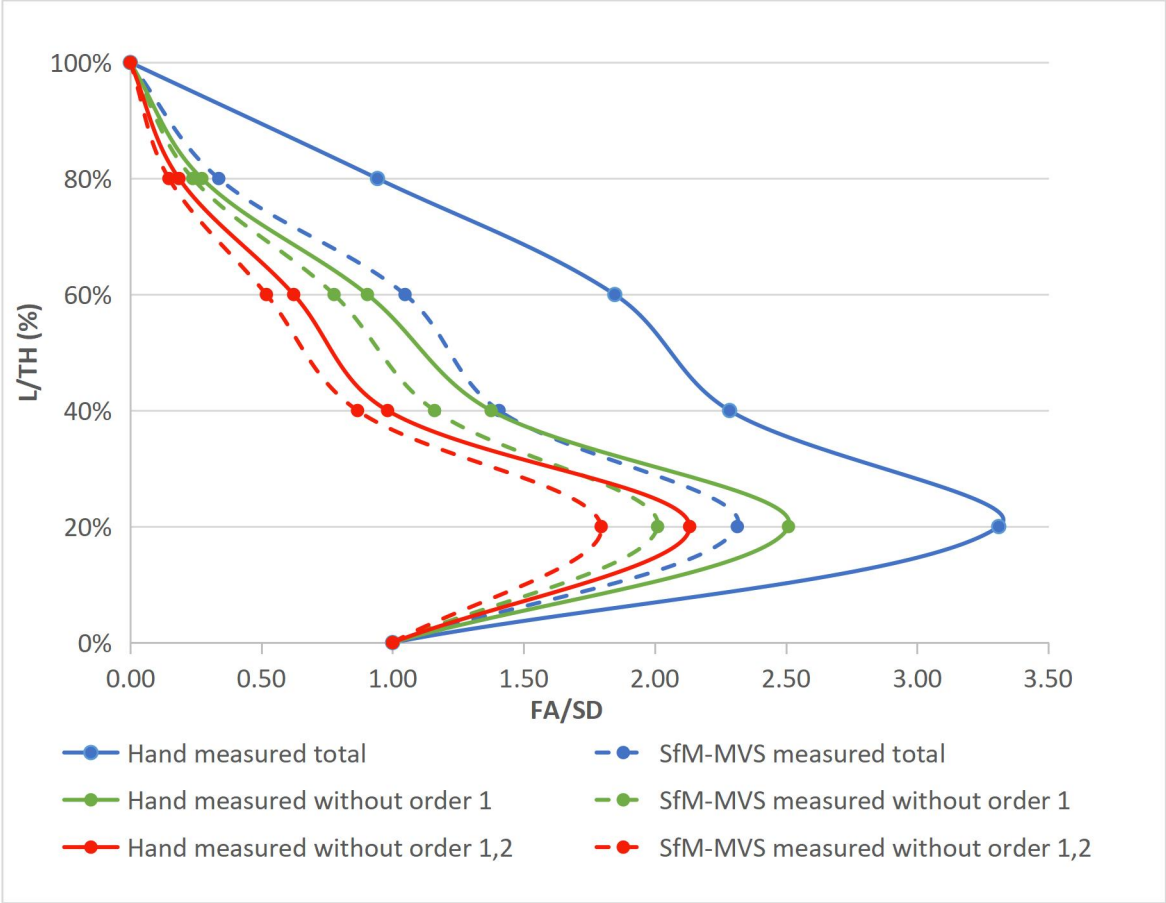

Figure 5.11. Gap of FA/SD between values estimated by smartphone-based SfM-MVS and the true values measured by the hand at various heights under different cases for all tree types. Y-axis (L/TH) means measured height divided by tree height, 0%-100% means from bottom to top for a tree.

The results of different types of trees are put together and averaged (data of 10 trees in total), and a general result is obtained, as shown in Figure 5.11. Similar conclusions can be drawn. The estimation error of FA/SD is greatly reduced after ignoring branches of 1st order. Branch orders above order 2 have a small effect on the accuracy of the FA/SD estimates. At this time, the distance between the solid line and the dashed line should be the FA/SD error caused by the smartphone-based SfM-MVS method itself.

6. Discussion and Recommendations

6.1. Optimal conditions for using smartphone-based SfM-MVS

According to the test of photography distance and ambient light intensity, the best photography distance we got is 25cm, and the most suitable outdoor weather condition is cloudy with no light condition. Due to the limited changes in the conditions set during the test and the variability of the actual field environment, the optimal conditions obtained here are approximate values, not exact values. Few previous studies have made a systematic introduction to how to perform SfM-MVS using a smartphone. Therefore, in order to critically evaluate our results, it is necessary to expand the range of comparisons, such as exploring the relative performance of traditional camera-based SfM-MVS and TLS methods.

In Olofsson et al. (2014), where TLS was used to measure tree parameters, RMSE initially increased with the distance of the tree from the scanner, but after removing outliers, there is no clear relationship between RMSE and distance. Liang et al. (2014) used a handheld camera to model trees in 3D, and proposed that the closer the object is to the photography path, the better the quality of point cloud generation, and the farthest photography distance is 15m. However, Liang et al. (2014) investigated large trees in the forest, and the different photography distances are set in a span of 5m, which is not consistent with the scope of this study.

Miller et al. (2015) after conducting a study of SfM-MVS using a hand-held camera, proposed that diffuse lighting is best, which reduces shadows and prevents direct sunlight from causing overexposed images. The cloudy and no-sunlight weather conditions obtained in this study are basically consistent with this. Bemis et al. (2014) and Gienko and Terry (2014) argued that images should be taken at an appropriate time (e.g. high noon sun) and within 30 minutes. Because the process is too long, the azimuth of the sun and the surface reflectivity will change greatly, which will affect the quality of the model. However, it is clear that the condition of high noon sun is not suitable for this study, which may be because they studied the SfM-MVS of large geological structures, while this study was aimed at small trees. The image acquisition time in this study was less than 30 minutes, same as in the cited study. Bemis et al. (2014) also suggested that taking pictures around reflective surfaces should be avoided. Additionally, Miller et al. (2015) proposed that photography in windy conditions should be avoided as much as possible, otherwise the wind will cause leaves and twigs to move. The greenhouse conditions in this study perfectly meet this requirement.

6.2. Linear estimation of smartphone-based SfM-MVS

The results of the error analysis show that the smartphone-based SfM-MVS achieves high accuracy for the estimation of the linear parameters of mangroves (tree height, canopy diameter,

stem diameter and diameter of branch with a high order). The RMSE of the estimated tree height is 13.51%, and the bias is -10.72%. And it has a very close linear relationship with the true value, with a R^2 of 0.9597. The main reason for the error may be the poor modeling of the small branches at the top of the tree. Some ground-based SfM-MVS studies can be used for critical evaluation. Miller et al. (2015) estimated tree parameters using SfM-MVS with a hand-held camera and found that the tree height RMSE was equal to 3.74%, with a bias of 1.74%, and R^2 value between the ground truth measurements of 0.982. Morgenroth and Gómez (2014) obtained an error of 2.59% in tree height for the commercial SfM-MVS test. The results of some studies using remote sensing techniques like TLS or ALS to obtain tree heights are also used for reference. Kankare et al. (2013) reported a tree height accuracy (RMSE%) of 8.05% for TLS estimation. Novotny et al. (2021) observed a strong correlation between spruce tree height and ground measurements after using TLS and ALS, respectively (r = 0.91-0.94 for ALS, r = 0.94 for TLS, r = 0.91), the standard error of estimation (SEE) ranged from 1.4 m to 2.2 m. In the study of Yin and Wang (2019), the TH of dwarf trees was overestimated with a bias of 3.5%-9.4% and an RMSE of 6.3%-14.3%. Wannasiri et al. (2013) obtained a R^2 value of 0.80 from LiDAR determination of tree height, an RMSE value of 1.42 m, and RE value of 19.2%. Among the best methods studied by Kaartinen et al. (2012), the measured accuracy of all types of tree heights after removing gross errors was better than 0.5 m. Jakubowski et al. (2013) used LIDAR data and WorldView-2 imagery to delineate individual tree heights, with high agreement between results and ground-measured data (R^2: 0.93-0.96). Ene et al. (2012) used ALS to measure individual tree parameters and found that tree height was systematically underestimated with an average error of 0.46-0.59. Shimizu et al. (2022) used TLS combined with aerial photography data and severely underestimated tree height, with an RMSE of 8.87 m (28.9%) and a bias of -8.39 m.

The estimated RMSE of canopy diameter in this study was 11.28%, with a bias of -8.71%. There was also a strong correlation between the estimated canopy diameter and the true value measured by hand, with a R^2 value of 0.8533 from the linear regression analysis. Similar to tree height, the error may be caused by poor resolution of the small branches at the ends of the canopy. For comparison, Miller et al. (2015) reported an estimated RMSE of 14.76% for true tree canopy spread (TCS) using SfM-MVS with a handheld camera. A study by Novotny et al. (2021) showed that the standard error of CD estimation using ALS was SEE = 1.2 m, and showed good linear relationship with field measurements (r = 0.71). Whereas the standard error of the CD estimate using TLS was SEE = 1.4 m, the linear relationship with the field measurements weakened (r = 0.52). Yin and Wang (2019) reported biass in canopy diameter estimates for dwarf trees of -0.16–0.60 m (-5.0%–19.9%), with RMSEs of 0.43–0.82 m (15.7%–27.5%). Wannasiri et al. (2013) measured canopy diameter using airborne LIDAR yielding a correlation coefficient R^2 of 0.75, an estimated root mean square error (RMSE) value of 1.65 m, and a relative error (RE) value of 19.7%.

Stem and branch diameters are discussed together. The RMSE for stem diameter (SD) was 2.06 mm (5.38%), with a bias of 2.12%, and the model estimate was extremely correlated with the measured value (R^2=9871). The RMSEs of the diameters of the two branches with different thicknesses were 4.78% and 7.41%, and the biass were 0% and -1.48%, respectively, and the model estimates of both parameters were highly correlated with the true values (R^2 were 0.9921

and 0.9643, respectively). It is clear that the smartphone-based SfM-MVS method achieved high accuracy in stem and branch diameter measurements, but the estimation error was larger for smaller diameter branches. The positive bias in stem diameter may be caused by the overlapping area of small roots around the stem. Stem diameter, branch diameter, or diameter at breast height (DBH) estimates from other literature can be used for comparison. In Miller et al. (2015), the DBH estimated RMSE was 2.11 mm (9.6%) with a R^2 of 0.935. Stem diameter was slightly less accurate than DBH, with an RMSE of 2.14 mm (11.93%). Fritz et al. (2013) used ground-based SfM-MVS to estimate the stem radius of different tree species with a Pearson correlation coefficient of r = 0.696. Morgenroth and Gómez (2014) used commercial SfM-MVS and obtained a stem diameter error of 3.7%. Olofsson et al. (2014) presented a TLS relative root mean square error (RMSE) of 14% for the estimated diameter at breast height. Liang et al. (2014) obtained an RMSE of 2.39 cm for DBH estimates for a single tree in a forest using a hand-held camera. The accuracy (RMSE%) of the high-precision TLS-derived DBH reported by Kankare et al. (2013) was 8.05%. Novotny et al. (2021) estimated DBH fort spruce and beech using hand-held TLS , got r = 0.96, with an average SEE of 2.9 cm. Shimizu et al. (2022) used the TLS method to achieve high accuracy for DBH estimation with a root mean square error (RMSE) of 2.36 cm (5.6%).

6.3. Smartphone-based SfM-MVS estimation of frontal area at a certain height

The frontal area here is also a 1D parameter, but instead of a single linear indicator, it includes the horizontal diameters of all branches at a certain height. Based on the tree height of each mangrove sample, we estimated the frontal area at four uniform heights. These 4 heights are called L1, L2, L3, L4 from low to high. The RMSE of the estimated mangrove frontal area at L1 was 36.35%, with a bias of -30.25%. The RMSE of the estimated frontal area at L2 was 41.47%, with a bias of -36.53%. The RMSE of the estimated frontal area at L3 was 46.41%, with a bias of -41.22%. The RMSE of the estimated frontal area at L4 was 76.39%, with a bias of -63.2%. Analyzing the frontal areas of the four heights together yielded a RMSE of 45.58% for the frontal area with a bias of -38.83%. And the linear regression analysis reported a strong linear relationship between the frontal area at a certain height and the true value by the hand measurement, R^2 is 0.8784. This result showed that the SfM-MVS model resulted in a large underestimation of the frontal area at each height. Since the value of RMSE and bias of the frontal area is the largest at L4, and trees usually contain more slender branches at L4 (the tallest of the 4 heights), we guess that the error was mainly determined by the proportion of thin branches at a certain height.

This conjecture was confirmed by the results of linear regression analysis of the proportion of frontal area occupied by branches with a diameter of 5 mm or less at a certain height and the absolute error of the estimated frontal area at this height. There is a high correlation between the two with R^2 of 0.8144. That is, the higher the proportion of the frontal area occupied by small branches with diameter <=5 mm at a certain height, the greater the error of the estimated frontal area at this height. This is also confirmed by the results of the resolution tests in Section 4.2,

which showed that the smartphone-based SfM-MVS model has very low resolution for branches with diameters <= 5 mm, and it's difficult to visualize then even in a good environmental condition, while branches with a diameter of more than 5mm can be modeled very well. In order to more intuitively feel the influence of small branches on the estimation of the frontal area at a certain height, this study explored the effect of branch order on the accuracy of FA/SD estimates over the height based on Jerez Nova (2022). It was demonstrated that branches with order 1 (smallest diameter) were the main cause of the larger error in the estimated FA/SD over the height. Here the branches with order 1 means their diameter <= 4mm. This result roughly agrees with the results of the linear regression analysis before (the resolution of branches below 5mm is very low). In order to improve the accuracy of the frontal area estimation, a correction factor of about 1.5 could be used (from Figure 5.11). Jerez Nova (2022) also suggested that the contribution of smaller tree branches to total frontal surface area is significant, as evidenced by the large frontal area error we got when considering all branches at a certain height.

Some related studies also report this problem. Miller et al. (2015) found poor reconstruction of point clouds with slender branches when reconstructing SfM-MVS models of trees using a hand-held camera, and introduced that this was caused by insufficient pixels in the image that could provide identifiable keypoints. The study also showed that in a canopy, branches are very slender (<5 mm) at their ends, and SfM-MVS is often unable to reconstruct the last 20-30 cm, thus causing errors in visible canopy spread and tree volume. The study of Morgenroth and Gómez (2014) confirmed that MVS is only effective for thick trunks, and the MVS process was unsuccessful because there were insufficient points in the point cloud representing the slender branches of the tree crown. By comparison, using smartphone-based SfM-MVS instead of traditional SfM-MVS still cannot effectively improve the resolution of branches with small diameters.

Another interesting aspect worth noting is that the flexibility of small branches may be helpful to the feasibility of using this method to measure the required tree frontal area. As discussed above, this method has defects in the accuracy of reconstructing the model of the small branches. However, in the actual field measurement work, small branches often deform under the action of current or waves, resulting in a significant reduction in the frontal area of small branches realated to wave damping. In other words, the frontal area of the branches with order 1 may have a limited effect on wave attenuation, especially under extreme conditions. This, to some extent, makes up for the shortcomings of this method in estimating the frontal area of mangroves. In order to verify this, more experiments and studies are needed.

6.4. Factors affecting the accuracy of the mangrove SfM-MVS model

There are many factors that can affect the accuracy of smartphone-based mangrove SfM-MVS models, and this study focused on testing the effects of photography distance and weather/light

conditions. The photography distance of around 25cm is better than 10cm and 50cm, which is reasonable. Because for smartphones, too close distance of photography will result in each photo containing very little tree structure and blurring the edge areas of the photo. Too far distance will result in insufficient pixels in the image, making the model less accurate. Cloudy with no sunlight condition is the best weather condition tested for this study. This is consistent with the diffuse light and preventing direct sunlight conditions proposed by Miller et al. (2015) . This environment can effectively reduce the leaf reflection and shadow area. But that doesn't mean that the darker the conditions, the better. For smartphones, a suitable ambient brightness is the basis for high-quality shots. This is also confirmed from the resolution tests in this study, where the resolution of the model was reduced for the darker conditions of 300 lux.

There are other potential factors that may also affect model accuracy. Such as insufficient overlap between consecutive photos or insufficient number of circular paths taken. In addition to the human error, this is mainly caused by the limitation of the number of pictures taken by the 'Polycam'. This study focused on mangrove individuals which are relatively low, so this problem did not arise. But if the same approach were applied to other species of trees that were taller, the problem would be magnified. Leaf area may also be an important factor in determining the accuracy of the mangrove SfM-MVS model. Because leaves have a limited role in the wave attenuation process (van Wesenbeeck et al., 2022) and are therefore not a important part of the model reconstruction. However, they can obscure tree branches and create a lot of shadow areas, which affects the quality of model reconstruction. The pixels of the device itself obviously also have a potential impact on the quality of the 3D model. Especially for branches with small diameters, increasing the pixels of the device can increase the key points that can be identified, thereby improving the quality of branch modeling. The iPhone 12 used in this study clearly still has room for improvement.

6.5. Recommendations

6.5.1. Best usage conditions tests

Since there are few previous studies using Polycam for 3D model reconstruction of mangroves. We therefore performed a series of tests to determine the optimal conditions for use of the method. But only one moderately sized tree sample was used for the experiment in the best photography distance test and the light intensity (weather) test. This is based on the assumption that the best use conditions for this tree represent the best use conditions for all other trees. But this has apparently not been confirmed. The experimental setup for the resolution test is also very simple and not rigorous enough. Therefore, for testing to determine the optimal conditions of use of the method, it is recommended that:

- Future research could test different species and sizes of trees to determine more detailed optimal use conditions.

- Test more different photography distances and more different light intensities
- Validation experiments can be carried out on trees of different species and sizes.
- Use the same species of trees to set up a more professional resolution test, and choose the same experimental site.

6.5.2. Accuracy improvement

This study analyzes the performance of the smartphone-based SfM-MVS method in estimating mangrove parameters related to wave attenuation. The results are generally satisfactory, especially for the estimation of tree height, canopy diameter, stem diameter and relatively thick branch diameter (all of the RMSEs are less than 15%). But there is still room for improvement in the future. The performance of the device and the mobile app itself will continue to improve with the advancement of technology. The iPhone 12 used in this study and the 3D modeling application 'Polycam' have room for improvement. The sample for this study was *Avicennia marina* vegetation, a tropical mangrove with dense foliage. Therefore, the occlusion of the leaves will affect the 3D reconstruction of the tree branch structure to a certain extent. At the same time, because the distance between two adjacent trees in the experimental greenhouse was not large enough, the model reconstruction of individual mangroves was affected by other mangrove individuals around it to a certain extent. Based on these issues, some methods that may further improve the accuracy of 3D models are listed as followed.

- Using mobile phones with higher pixels can capture small structures more clearly.
- In the future, applications that are more suitable than 'Polycam' for 3D model reconstruction of trees may be used.
- For deciduous plants, we can choose to collect images during the deciduous period to reduce the impact of leaves on the accuracy.
- For evergreen plants, some technical means can be used to separate the branches and leaves of the three-dimensional point cloud of trees, so as to remove the leaves and facilitate the measurement.
- Minimize the complexity of the environment around the target tree sample, such as using cardboard to block around the sample.
- Minimize reflective light sources near the sample trees, such as water surfaces, glass, etc.
- A correction factor (about 1.5) may be used for the estimation of frontal area.

It is worth noting that if some technical methods are used to separate the branches and leaves of the 3D point cloud of trees, it is necessary to avoid the secondary error caused by the technical methods itself. For example, if a kind of method will remove some branches along with leaves, the pros and cons need to be carefully considered.

6.5.3. Limitation of smartphone-based SfM-MVS

The smartphone-based SfM-MVS method itself has some limitations. The limitation of the number of photos taken by the mobile phone application makes the objects reconstructed by the model cannot cover more details. This method also has strict requirements on the environment, changes in light intensity and photography distance will greatly affect the quality of the model. In order to achieve good model reconstruction quality, the size of the trees is also limited. In addition, as discussed in Section 6.3, the flexibility of small branches may improve the feasibility of this method in practical application and the accuracy of measurement. Based on these current situations, some suggestions for using the smartphone-based SfM-MVS method for trees are as follows:

- Keeping the most suitable photography distance and light intensity for image acquisition.
- The size of the target tree should not be too large, preferably low shrubs.
- Under extreme conditions, the feasibility of this method in estimating mangrove frontal area may be improved.

7. Conclusions

This chapter summarizes the findings of this study. The answers to the research questions (see Section 1.2.1 for details) are presented in this chapter. The purpose of this study is to explore the feasibility of smartphone-based structure-from-motion with multi-view stereo-photogrammetry (SfM-MVS) for obtaining mangrove parameters related to wave damping. To achieve this, we answered the following sub-questions:

What are the relevant mangrove parameters for wave damping?

The results of literature study showed that wave attenuation caused by vegetation mainly depends on hydraulic conditions and vegetation parameters. There are many relevant vegetation parameters, such as canopy density, geometric features, stiffness, vegetation height, and vegetation frontal area. For rigid vegetation, the frontal area is one of the main parameters related to wave attenuation. Based on this, this study selected the geometric linear characteristics of mangroves (tree height, canopy diameter, stem diameter and branch diameter) and the frontal area at a certain height as the parameter targets.

How to use smartphone-based SfM-MVS to obtain the parameters?

In this study, iPhone 12 with application 'Polycam' were selected as image acquisition devices. During the process of image acquisition, it is necessary to maintain a smooth, slow and even moving of device, and cover every structure of the individual tree as much as possible (at least 3

circular paths through top-middle-bottom). After the image is collected and uploaded, Polycam will automatically complete the SfM-MVS process according to its own algorithm to obtain a reconstructed 3D model. Finally, the model is exported to Cloudcompare in point cloud format for processing and parameter measurement.

What is the optimal condition to use smartphone-based SfM-MVS for mangrove ?

In this study, the best photography distance obtained after testing is about 25cm, and the best weather condition is cloudy with no light condition. Under this condition, the accuracy of mangrove parameters reached the highest. It should be noted, however, this condition does not necessarily apply to different types of vegetation in other environments.

What is the accuracy of the mangrove parameter estimates using this method?

The results of the error analysis show that the smartphone-based SfM-MVS achieves high accuracy for the estimation of the linear parameters of mangroves (tree height, canopy diameter, stem diameter and diameter of branch with a high order). The RMSE of the estimated tree height is 13.51%, and the bias is -10.72%. And it has a very close linear relationship with the true value, with a R^2 of 0.9597. The estimated RMSE of canopy diameter in this study was 11.28%, with a bias of -8.71%. There was also a strong correlation between the estimated canopy diameter and the true value measured by hand, with a R^2 value of 0.8533 from the linear regression analysis. The RMSE for stem diameter (SD) was 2.06 mm (5.38%), with a bias of 2.12%, and the model estimate was extremely correlated with the measured value (R^2=9871). The RMSEs of the diameters of the two branches with different thicknesses were 4.78% and 7.41%, and the biass were 0% and -1.48%, respectively, and the model estimates of both parameters were highly correlated with the true values (R^2 were 0.9921 and 0.9643, respectively).

Based on the tree height of each mangrove sample, we also estimated the frontal area at four uniform heights. These 4 uniform heights are called L1, L2, L3, L4 from low to high. The RMSE of the estimated mangrove frontal area at L1 was 36.35%, with a bias of -30.25%. The RMSE of the estimated frontal area at L2 was 41.47%, with a bias of -36.53%. The RMSE of the estimated frontal area at L3 was 46.41%, with a bias of -41.22%. The RMSE of the estimated frontal area at L4 was 76.39%, with a bias of -63.2%. Analyzing the frontal areas of the four heights together yielded a RMSE of 45.58% for the frontal area with a bias of -38.83%. And the linear regression analysis reported a tight linear relationship between the frontal area at a certain height and the true value by the hand measurement, R^2 is 0.8784. This result showed that the SfM-MVS model resulted in a large underestimation of the frontal area at each height.

What factors could affect the accuracy of mangrove parameter estimates using this method?

The branch size is an important limiting factor for the model accuracy. In this studt, the effects of branch diameter and branch order on the accuracy of estimates of mangrove frontal area at a certain height were analyzed separately. The results show that (see Figures 5.7 and 5.8), at a certain height, the proportion of frontal area occupied by branches with a diameter of 5 mm or less has a strong positive correlation with the error of the estimated frontal area. The presence of the lowest order branches (order 1) is the main cause of the large error between the estimated and true value of the frontal area at a height. The results of the resolution tests on branches with different diameters can also confirm this point: the resolution of the method for branches with a diameter of less than 5mm is very low, and even under optimal environmental conditions, branches with a diameter of less than 5mm are difficult to appear in the reconstructed 3D model. The above analysis results show that branches with small diameters and orders are the main cause of relatively large errors in the estimated frontal area at a certain height. Extreme conditions may compensate for this limitation, because the flexibility of small branches could cause the reduction of their actual frontal area during wave attenuation.

Besides, the accuracy of the smartphone-based SfM-MVS method itself is also affected by some factors. Taking photos too far and too close will reduce accuracy. Too much or too little light intensity can also reduce the accuracy of the method. There are also potential factors that may affect accuracy to some extent. For example, the quality of the equipment will have a certain impact. Improper human manipulation during image acquisition can also affect the quality of the model. Occlusion by tree leaves reduces the accuracy of parameter measurements. The presence of wind and ambient reflected light can also adversely affect model quality and reduce the accuracy of parameter measurements.

How to correct and improve this technique?

- Selecting more samples for more detailed environmental testing to obtain a better operating condition.
- In the future, choosing mobile devices with better pixels and better 3D modeling applications for smartphones.
- More samples can be selected to test the accuracy and feasibility of this technique in more parameter measurements. For parameters that cannot be accurately measured using this technique, other methods can be used to compensate.
- Testing more samples, summarizing more data, and finding general patterns of the effect of different orders of branches on the measurement error of frontal area at different heights.

The main research question in this study:
Is it feasible to determine relevant mangrove parameters for wave damping using a smartphone-based SfM-MVS approach?

It is feasible to estimate mangrove parameters related to wave attenuation using the smartphone-based SfM-MVS method. Among them, for tree height, canopy diameter, stem

diameter and thick branch diameter, the method achieves high-accuracy estimation. For the frontal area at a certain height, there is a related big error in the estimated value of this method, which is mainly caused by the insufficient resolution of the method for thin branches with a diameter of less than 5mm at the end of the tree. Some potential factors may make up for this defect to some extent and improve the possibility of practical application of this method.The smartphone-based SfM-MVS measurement method for tree parameters is not yet mature, there is still a lot of room for improvement at this stage.

Bibliography

Antonarakis, A. S., et al. "Leafless roughness of complex tree morphology using terrestrial lidar." Water Resources Research 45.10 (2009).

Bouma, T. J., et al. "Trade-offs related to ecosystem engineering: A case study on stiffness of emerging macrophytes." Ecology 86.8 (2005): 2187-2199.

Bragg, Don C. "An improved tree height measurement technique tested on mature southern pines." Southern Journal of Applied Forestry 32.1 (2008): 38-43.

Corradetti, Amerigo, et al. "Virtual outcrops in a pocket: The smartphone as a fully equipped photogrammetric data acquisition tool." GSA TODAY 31.9 (2021): 4-9.

Dalrymple, Robert A., James T. Kirby, and Paul A. Hwang. "Wave diffraction due to areas of energy dissipation." Journal of waterway, port, coastal, and ocean engineering 110.1 (1984): 67-79.

Douglas, Ian, et al. "Unjust waters: climate change, flooding and the urban poor in Africa." Environment and urbanization 20.1 (2008): 187-205.

Ene, Liviu, Erik Næsset, and Terje Gobakken. "Single tree detection in heterogeneous boreal forests using airborne laser scanning and area-based stem number estimates." International Journal of Remote Sensing 33.16 (2012): 5171-5193.

Etminan, Vahid, Ryan J. Lowe, and Marco Ghisalberti. "Canopy resistance on oscillatory flows." Coastal Engineering 152 (2019): 103502.

Fisher, Robert B., et al. Dictionary of computer vision and image processing. John Wiley & Sons, 2013.

Guo, Yasong, et al. "New morphological features for urban tree species identification using LiDAR point clouds." Urban Forestry & Urban Greening 71 (2022): 127558.

Gollob, Christoph, et al. "Measurement of forest inventory parameters with Apple iPad pro and integrated LiDAR technology." Remote Sensing 13.16 (2021): 3129.

Hochard, J. P., Hamilton, S. & Barbier, E. B. Mangroves shelter coastal economic activity from cyclones. https://doi.org/10.1073/ pnas.1820067116 (2019).

Horstman E M, Dohmen-Janssen C M, Narra P M F, et al. Wave attenuation in mangroves: A quantitative approach to field observations[J]. Coastal engineering, 2014, 94: 47-62.

Hu, Z., Suzuki, T., Zitman, T., Uittewaal, W., and Stive, M. (2014). Laboratory study on wave dissipation by vegetation in combined current-wave flow. Coastal Eng. 88, 131–142. doi: 10.1016/j.coastaleng.2014.02.009

Heinzel J, Huber M O. Tree stem diameter estimation from volumetric tls image data[J]. Remote Sensing, 2017, 9(6): 614.

Holopainen M, Vastaranta M, Kankare V, et al. Mobile terrestrial laser scanning in urban tree inventory[C]//Proceedings of 11th International Conference on LiDAR Applications for Assessing Forest Ecosystems (SilviLaser 2011), Hobart, Australia. 2011, 1620: 17.

Indirabai I, Nair M V H, Jaishanker R N, et al. Terrestrial laser scanner based 3D reconstruction of trees and retrieval of leaf area index in a forest environment[J]. Ecological Informatics, 2019, 53: 100986.

Jakubowski, Marek K., et al. "Delineating individual trees from LiDAR data: A comparison of vector-and raster-based segmentation approaches." Remote Sensing 5.9 (2013): 4163-4186.

James, Michael R., and Stuart Robson. "Straightforward reconstruction of 3D surfaces and topography with a camera: Accuracy and geoscience application." Journal of Geophysical Research: Earth Surface 117.F3 (2012).

Järvelä, Juha. "Determination of flow resistance caused by non-submerged woody vegetation." International Journal of River Basin Management 2.1 (2004): 61-70.

Jaud, Marion, et al. "Potential of smartphone SfM photogrammetry to measure coastal morphodynamics." Remote Sensing 11.19 (2019): 2242.

Kalloe S A, Hofland B, Antolínez J A A, et al. Quantifying Frontal-Surface Area of Woody Vegetation: A Crucial Parameter for Wave Attenuation[J]. Frontiers in Marine Science, 2022, 9: 820846.

Kelty K, Tomiczek T, Cox D T, et al. Prototype-scale physical model of wave attenuation through a mangrove forest of moderate cross-shore thickness: LiDAR-based characterization and Reynolds scaling for engineering with nature[J]. Frontiers in Marine Science, 2022: 2044.

Kankare, Ville, et al. "Individual tree biomass estimation using terrestrial laser scanning." ISPRS Journal of Photogrammetry and Remote Sensing 75 (2013): 64-75.

Kaartinen, Harri, et al. "An international comparison of individual tree detection and extraction using airborne laser scanning." Remote Sensing 4.4 (2012): 950-974.

Koch, Evamaria W., et al. "Non-linearity in ecosystem services: temporal and spatial variability in coastal protection." Frontiers in Ecology and the Environment 7.1 (2009): 29-37.

Kobayashi, Nobuhisa, Andrew W. Raichle, and Toshiyuki Asano. "Wave attenuation by vegetation." Journal of waterway, port, coastal, and ocean engineering 119.1 (1993): 30-48.

Liang, Xinlian, et al. "The use of a hand-held camera for individual tree 3D mapping in forest sample plots." Remote Sensing 6.7 (2014): 6587-6603.

Luetzenburg, Gregor, Aart Kroon, and Anders A. Bjørk. "Evaluation of the Apple iPhone 12 Pro LiDAR for an application in geosciences." Scientific reports 11.1 (2021): 1-9.

Lou S, Chen M, Ma G, et al. Laboratory study of the effect of vertically varying vegetation density on waves, currents and wave-current interactions[J]. Applied Ocean Research, 2018, 79: 74-87.

McGranahan, G., Balk, D. & Anderson, B. The rising tide: assessing the risks of climate change and human settlements in low elevation coastal zones. Environ. Urban. 19, 17–37 (2007).

Menéndez, P., Losada, I.J., Torres-Ortega, S. et al. The Global Flood Protection Benefits of Mangroves. Sci Rep 10, 4404 (2020). https://doi.org/10.1038/s41598-020-61136-6

Mendez F J, Losada I J. An empirical model to estimate the propagation of random breaking and nonbreaking waves over vegetation fields[J]. Coastal Engineering, 2004, 51(2): 103-118.

Maza M, Lara J L, Losada I J. Predicting the evolution of coastal protection service with mangrove forest age[J]. Coastal Engineering, 2021, 168: 103922.

Mcivor, A., Spencer, T. & Möller, I. Storm Surge Reduction by Mangroves. Nat. Coast. Prot. Ser. 35 ISSN 2050-7941 (2012).

Miller J, Morgenroth J, Gomez C. 3D modelling of individual trees using a handheld camera: Accuracy of height, diameter and volume estimates[J]. Urban Forestry & Urban Greening, 2015, 14(4): 932-940.

Marchi, Niccolò, Francesco Pirotti, and Emanuele Lingua. "Airborne and terrestrial laser scanning data for the assessment of standing and lying deadwood: Current situation and new perspectives." Remote Sensing 10.9 (2018): 1356.

Maltamo, Matti, Erik Næsset, and Jari Vauhkonen. "Forestry applications of airborne laser scanning." Concepts and case studies. Manag For Ecosys 27 (2014): 460.

Maza, Maria, Javier L. Lara, and Iñigo J. Losada. "Experimental analysis of wave attenuation and drag forces in a realistic fringe Rhizophora mangrove forest." Advances in Water Resources 131 (2019): 103376.

Mendez, Fernando J., and Inigo J. Losada. "An empirical model to estimate the propagation of random breaking and nonbreaking waves over vegetation fields." Coastal Engineering 51.2 (2004): 103-118.

Morison, J. R., J. W. Johnson, and S. A. Schaaf. "The force exerted by surface waves on piles." Journal of Petroleum Technology 2.05 (1950): 149-154.

Mokroš, Martin, et al. "Novel low-cost mobile mapping systems for forest inventories as terrestrial laser scanning alternatives." International Journal of Applied Earth Observation and Geoinformation 104 (2021): 102512.

Moore A W. An intoductory tutorial on kd-trees[J]. 1991.

Miller, Jordan Mitchell. "Estimation of individual tree metrics using structure-from-motion photogrammetry." (2015).

Morgenroth, J., and Ch Gómez. "Assessment of tree structure using a 3D image analysis technique—A proof of concept." Urban Forestry & Urban Greening 13.1 (2014): 198-203.

McMahon, Thomas A., and Richard E. Kronauer. "Tree structures: deducing the principle of mechanical design." Journal of theoretical biology 59.2 (1976): 443-466.

Novotny J, Navratilova B, Albert J, et al. Comparison of spruce and beech tree attributes from field data, airborne and terrestrial laser scanning using manual and automatic methods[J]. Remote Sensing Applications: Society and Environment, 2021, 23: 100574.

Olofsson, Kenneth, Johan Holmgren, and Håkan Olsson. "Tree stem and height measurements using terrestrial laser scanning and the RANSAC algorithm." Remote sensing 6.5 (2014): 4323-4344.

Phan, K. L., et al. "The effects of wave non-linearity on wave attenuation by vegetation." Coastal Engineering 147 (2019): 63-74.

Paul M, Rupprecht F, Möller I, et al. Plant stiffness and biomass as drivers for drag forces under extreme wave loading: a flume study on mimics[J]. Coastal Engineering, 2016, 117: 70-78.

Robertson and Cipolla. "Structure from motion" M. Varga (Ed.), Practial Image Processing and Computer Vision, John Wiley and Sons, New York (2009)

Sarpkaya, Turgut, and Michael Isaacson. Mechanics of wave forces on offshore structures. New York (NY): Van Nostrand Reinhold, 1981., 1981.

Strahler, A. N. "The Nature of Induced Erosion and Aggradation in: WL Thomas' Man's Role in Changing the Face of the Earth." (1956): 621-638.

Shimizu K, Nishizono T, Kitahara F, et al. Integrating terrestrial laser scanning and unmanned aerial vehicle photogrammetry to estimate individual tree attributes in managed coniferous forests in Japan[J]. International Journal of Applied Earth Observation and Geoinformation, 2022, 106: 102658.

S. L. Tran Kai Frank Da and M. Yvinec. CGAL 4.14 3d alpha shapes, 2019. URL https://doc.cgal.org/latest/Alpha_shapes_3/index.html#title3.

Szeliski, Richard. Computer vision: algorithms and applications. Springer Nature, 2022.
Smith, Mark William, Jonathan L. Carrivick, and Duncan J. Quincey. "Structure from motion photogrammetry in physical geography." Progress in physical geography 40.2 (2016): 247-275.

Suzuki, T., Zijlema, M., Burger, B., Meijer, M. C. & Narayan, S. Wave dissipation by vegetation with layer schematization in SWAN. Coast. Eng. 59, 64–71 (2012).

Tavani S, Billi A, Corradetti A, et al. Smartphone assisted fieldwork: Towards the digital transition of geoscience fieldwork using LiDAR-equipped iPhones[J]. Earth-Science Reviews, 2022: 103969.

Tschirky, Paul, Kevin Hall, and David Turcke. "Wave attenuation by emergent wetland vegetation." Coastal Engineering 2000. 2001. 865-877.
Tampanya, U., Vermaat, J. E., Sinsakul, S. & Panapitukkul, N. Coastal erosion and mangrove progradation of Southern Tailand. Estuar. Coast. Shelf Sci. 68, 75–85 (2006).

van Zelst, V.T.M., Dijkstra, J.T., van Wesenbeeck, B.K. et al. Cutting the costs of coastal protection by integrating vegetation in flood defences. Nat Commun 12, 6533 (2021). https://doi.org/10.1038/s41467-021-26887-4

van Wesenbeeck, B.K., Wolters, G., Antolínez, J.A.A. et al. Wave attenuation through forests under extreme conditions. Sci Rep 12, 1884 (2022). https://doi.org/10.1038/s41598-022-05753-3

van Hespen R, Hu Z, Peng Y, et al. Analysis of coastal storm damage resistance in successional mangrove species[J]. Limnology and Oceanography, 2021, 66(8): 3221-3236.

Vo-Luong, P., and Massel, S. (2008). Energy dissipation in non-uniform mangrove forests of arbitrary depth. J. Mar. Syst. 74, 603–622. doi: 10.1016/j.jmarsys.2008.05.004

Westoby, Matthew J., et al. "'Structure-from-Motion'photogrammetry: A low-cost, effective tool for geoscience applications." Geomorphology 179 (2012): 300-314.

Westoby, Matthew J., et al. "'Structure-from-Motion'photogrammetry: A low-cost, effective tool for geoscience applications." Geomorphology 179 (2012): 300-314.

Wannasiri, Wasinee, et al. "Extraction of mangrove biophysical parameters using airborne LiDAR." Remote Sensing 5.4 (2013): 1787-1808.

Yamamoto, Hiroyuki, Masato Yoshida, and Takashi Okuyama. "Growth stress controls negative gravitropism in woody plant stems." Planta 216.2 (2002): 280-292.

Yao, Tian, et al. "Measuring forest structure and biomass in New England forest stands using Echidna ground-based lidar." Remote sensing of Environment 115.11 (2011): 2965-2974.

Yin D, Wang L. Individual mangrove tree measurement using UAV-based LiDAR data: Possibilities and challenges[J]. Remote Sensing of Environment, 2019, 223: 34-49.

Ysebaert, Tom, et al. "Wave attenuation by two contrasting ecosystem engineering salt marsh macrophytes in the intertidal pioneer zone." Wetlands 31.6 (2011): 1043-1054.

Zhang, Wei, et al. "The role of seasonal vegetation properties in determining the wave attenuation capacity of coastal marshes: Implications for building natural defenses." Ecological Engineering 175 (2022): 106494.

Appendix

A. Background information

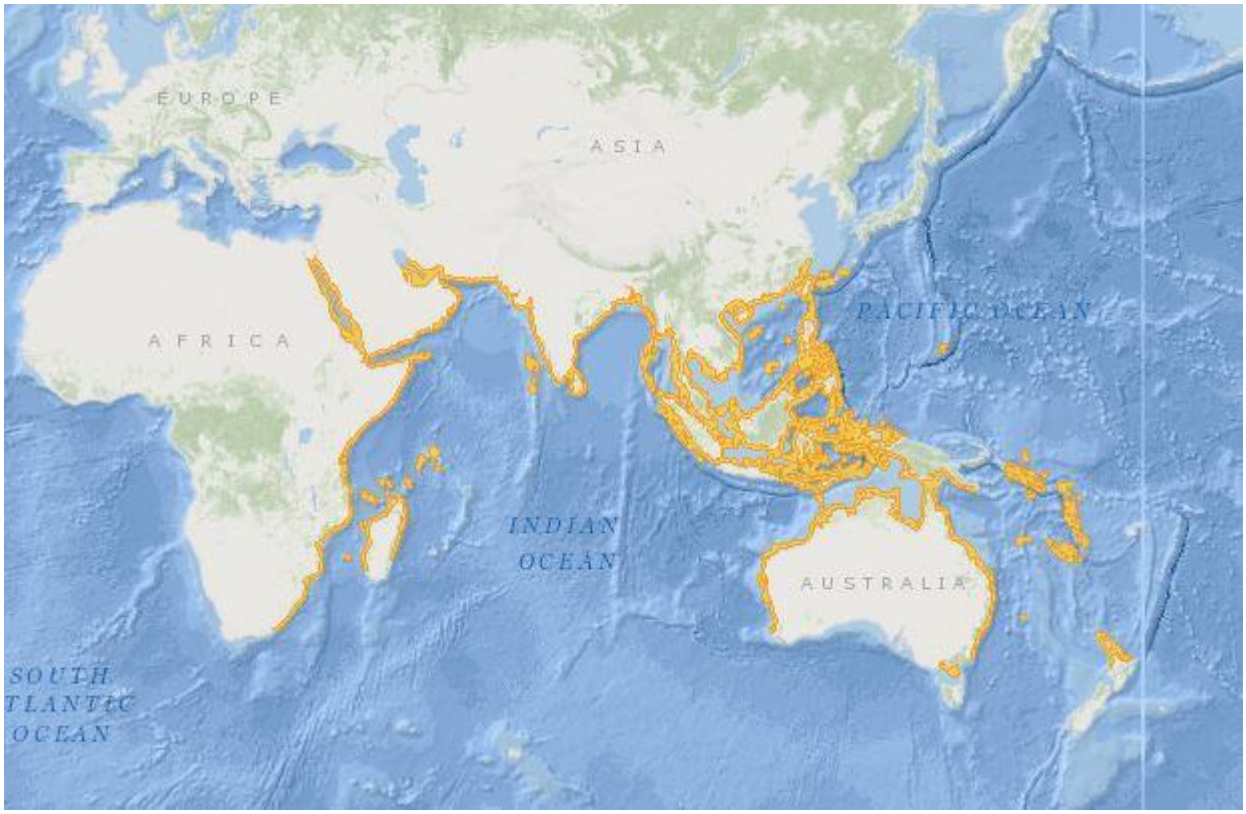

Figure A.1. Global distribution of Avicennia marina vegetation (mangrove) used in this study.

B. Mangrove samples

Box31

Box30

Box28

Box23

Box14

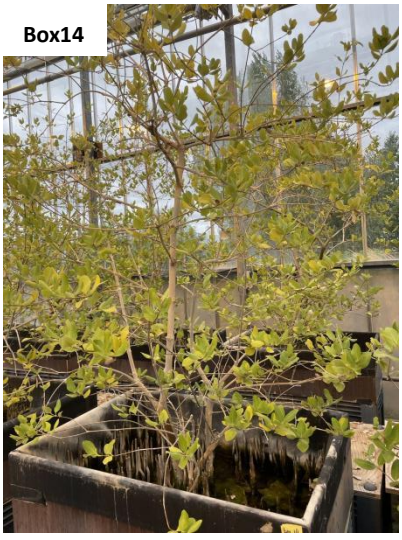

Box16

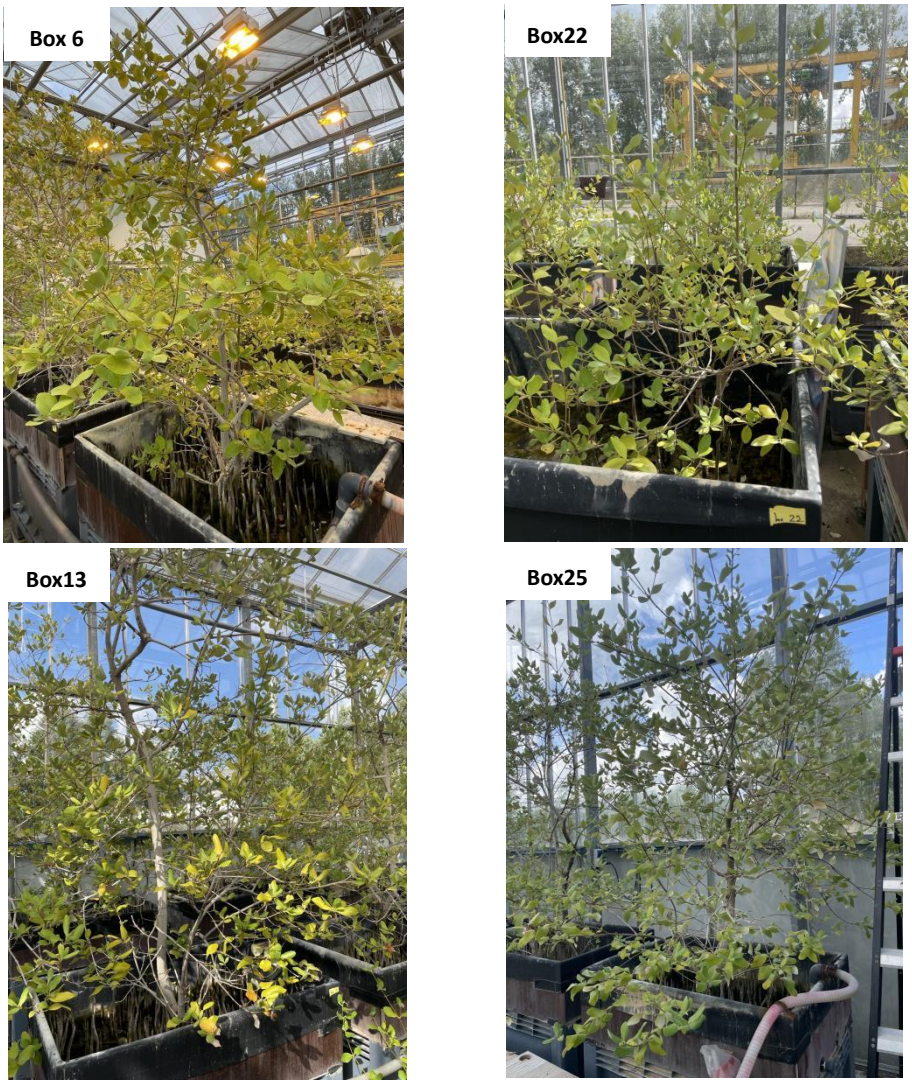

Figure B.1. 10 mangrove samples measured in the report.

C. Smartphone-based SfM-MVS measurement

Box31			
Metric	Measured	Modelled	Error
Tree height(mm)	1440	1421	-1.32%
Canopy diameter(mm)	1185	1225	3.38%
Stem diameter(mm)	24.5	23.9	-2.45%
Branch diameter 1(mm)	7.5	7.2	-4.00%
Branch diameter 2(mm)	5	4.6	-8.00%
Frontal area at L1(mm)	133	61	-54.14%
Frontal area at L2(mm)	90	48	-46.67%
Frontal area at L3(mm)	51	14	-72.55%
Frontal area at L4(mm)	18	3	-83.33%

Box30			
Metric	Measured	Modelled	Error
Tree height(mm)	2180	1967	-9.77%
Canopy diameter(mm)	1450	1246	-14.07%
Stem diameter(mm)	54	55.1	2.04%
Branch diameter 1(mm)	21	19.9	-5.24%
Branch diameter 2(mm)	9	8.2	-8.89%
Frontal area at L1(mm)	43	40.5	-5.81%
Frontal area at L2(mm)	53	41	-22.64%
Frontal area at L3(mm)	120	75	-37.50%
Frontal area at L4(mm)	42	16	-61.90%

Box28			
Metric	Measured	Modelled	Error
Tree height(mm)	1780	1607	-9.72%
Canopy diameter(mm)	1110	1038	-6.49%
Stem diameter(mm)	38	40	5.26%
Branch diameter 1(mm)	14	15.1	7.86%
Branch diameter 2(mm)	10	9.3	-7.00%
Frontal area at L1(mm)	65	57	-12.31%
Frontal area at L2(mm)	37	25	-32.43%
Frontal area at L3(mm)	34	24	-29.41%
Frontal area at L4(mm)	59	34	-42.37%

Box23			
Metric	Measured	Modelled	Error
Tree height(mm)	1400	1243	-11.21%
Canopy diameter(mm)	1170	981	-16.15%
Stem diameter(mm)	37	36.6	-1.08%
Branch diameter 1(mm)	20	20.7	3.50%
Branch diameter 2(mm)	11	9.6	-12.73%
Frontal area at L1(mm)	90	66	-26.67%
Frontal area at L2(mm)	97	32	-67.01%
Frontal area at L3(mm)	31	10	-67.74%
Frontal area at L4(mm)	11	0	-100.00%

Box14			
Metric	Measured	Modelled	Error
Tree height(mm)	2140	1843	-13.88%
Canopy diameter(mm)	1540	1332	-13.51%
Stem diameter(mm)	29	29.5	1.72%
Branch diameter 1(mm)	23	22.1	-3.91%
Branch diameter 2(mm)	10	11.1	11.00%
Frontal area at L1(mm)	166	127	-23.49%
Frontal area at L2(mm)	91	73	-19.78%
Frontal area at L3(mm)	89	63	-29.21%
Frontal area at L4(mm)	44	19	-56.82%

Box16			
Metric	Measured	Modelled	Error
Tree height(mm)	850	822	-3.29%
Canopy diameter(mm)	1120	1090	-2.68%
Stem diameter(mm)	24	23.1	-3.75%
Branch diameter 1(mm)	13	11.6	-10.77%
Branch diameter 2(mm)	9.5	10	5.26%
Frontal area at L1(mm)	29	25	-13.79%
Frontal area at L2(mm)	61	45	-26.23%
Frontal area at L3(mm)	45	22	-51.11%
Frontal area at L4(mm)	10	2	-80.00%

Box6			
Metric	Measured	Modelled	Error
Tree height(mm)	1800	1767	-1.83%
Canopy diameter(mm)	1360	1346	-1.03%
Stem diameter(mm)	45	47.3	5.11%
Branch diameter 1(mm)	27	28	3.70%
Branch diameter 2(mm)	16	15.6	-2.50%
Frontal area at L1(mm)	153	106	-30.72%
Frontal area at L2(mm)	94	70	-25.53%
Frontal area at L3(mm)	62	41	-33.87%
Frontal area at L4(mm)	52	21	-59.62%

Box22			
Metric	Measured	Modelled	Error
Tree height(mm)	1250	1019	-18.48%
Canopy diameter(mm)	980	904	-7.76%
Stem diameter(mm)	21	22.1	5.24%
Branch diameter 1(mm)	15.5	14.9	-3.87%
Branch diameter 2(mm)	6.5	5.8	-10.77%
Frontal area at L1(mm)	152	118	-22.37%
Frontal area at L2(mm)	55	20	-63.64%
Frontal area at L3(mm)	19.5	9	-53.85%
Frontal area at L4(mm)	7	0	-100.00%

Box13			
Metric	Measured	Modelled	Error
Tree height(mm)	2900	2365	-18.45%
Canopy diameter(mm)	1450	1320	-8.97%
Stem diameter(mm)	62	67	8.06%
Branch diameter 1(mm)	42	41.5	-1.19%
Branch diameter 2(mm)	18	18.2	1.11%
Frontal area at L1(mm)	132	81	-38.64%
Frontal area at L2(mm)	97	66	-31.96%
Frontal area at L3(mm)	138	85	-38.41%
Frontal area at L4(mm)	108	40	-62.96%

Bx25			
Metric	Measured	Modelled	Error
Tree height(mm)	2130	1900	-10.80%
Canopy diameter(mm)	1780	1518	-14.72%
Stem diameter(mm)	48	46	-4.17%
Branch diameter 1(mm)	40	42	5.00%
Branch diameter 2(mm)	13	14	7.69%
Frontal area at L1(mm)	146	92	-36.99%
Frontal area at L2(mm)	127	89	-29.92%
Frontal area at L3(mm)	142	87	-38.73%
Frontal area at L4(mm)	43	10	-76.74%

Figure C.1. Error analysis for 10 mangroves.

Box31							
Measured	FA total	FA order 1	FA order 2	FA order 3	FA order 4		
Height L1	133	60	43	12	18		
Height L2	90	51	17	22	0		
Height L3	51	39	12	0	0		
Height L4	18	18	0	0	0		
Modelled	FA total	FA order 1	FA order 2	FA order 3	FA order 4		
Height L1	61	15	23	6	17		
Height L2	48	12	14	22	0		
Height L3	14	6	8	0	0		
Height L4	3	3	0	0	0		
Box30							
Measured	FA total	FA order 1	FA order 2	FA order 3	FA order 4	FA order 5	
Height L1	43	0	5	0	38	0	
Height L2	53	9	0	25	19	0	
Height L3	120	60	0	60	0	0	
Height L4	42	32	10	0	0	0	
Modelled	FA total	FA order 1	FA order 2	FA order 3	FA order 4	FA order 5	
Height L1	40.5	0	5.5	0	35	0	
Height L2	41	0	0	23	18	0	
Height L3	75	28	5	42	0	0	
Height L4	16	11	5	0	0	0	
Box28							
Measured	FA total	FA order 1	FA order 2	FA order 3	FA order 4	FA order 5	
Height L1	65	12	12	20	21	0	
Height L2	37	15	5	0	17	0	
Height L3	34	8	12	0	14	0	
Height L4	59	35	10	0	14	0	
Modelled	FA total	FA order 1	FA order 2	FA order 3	FA order 4	FA order 5	
Height L1	57	13	13	9	22	0	
Height L2	25	7	5	13	0	0	
Height L3	24	0	0	10	14	0	
Height L4	34	7	11	0	16	0	

Box23							
Measured	FA total	FA order 1	FA order 2	FA order 3	FA order 4	FA order 5	
Height L1	90	48	6	36	0	0	
Height L2	97	79	18	0	0	0	
Height L3	31	26	5	0	0	0	
Height L4	11	11	0	0	0	0	
Modelled	FA total	FA order 1	FA order 2	FA order 3	FA order 4	FA order 5	
Height L1	66	28	6	32	0	0	
Height L2	32	16	16	0	0	0	
Height L3	10	10	0	0	0	0	
Height L4	0	0	0	0	0	0	
Box14							
Measured	FA total	FA order 1	FA order 2	FA order 3	FA order 4	FA order 5	FA order 6
Height L1	166	21	10	16	0	60	59
Height L2	91	16	6	0	14	55	0
Height L3	89	32	13	9	0	35	0
Height L4	44	26	0	18	0	0	0
Modelled	FA total	FA order 1	FA order 2	FA order 3	FA order 4	FA order 5	FA order 6
Height L1	127	6	7	20	0	25	69
Height L2	73	8	7	0	0	18	40
Height L3	63	6	23	0	0	0	34
Height L4	19	0	6	13	0	0	0
Box16							
Measured	FA total	FA order 1	FA order 2	FA order 3	FA order 4		
Height L1	29	2	0	0	27		
Height L2	61	13	14	14	20		
Height L3	45	32	4	9	0		
Height L4	10	10	0	0	0		
Modelled	FA total	FA order 1	FA order 2	FA order 3	FA order 4		
Height L1	25	0	0	0	25		
Height L2	45	3	9	13	20		
Height L3	22	9	5	8	0		
Height L4	2	2	0	0	0		

Box6							
Measured	FA total	FA order 1	FA order 2	FA order 3	FA order 4	FA order 5	FA order 6
Height L1	153	33	26	10	37	20	27
Height L2	94	24	12	26	11	21	0
Height L3	62	18	12	0	12	20	0
Height L4	52	32	10	10	0	0	0
Modelled	FA total	FA order 1	FA order 2	FA order 3	FA order 4	FA order 5	FA order 6
Height L1	106	10	7	28	11	23	27
Height L2	70	13	17	20	0	20	0
Height L3	41	3	5	0	12	21	0
Height L4	21	2	10	9	0	0	0
Box22							
Measured	FA total	FA order 1	FA order 2	FA order 3	FA order 4		
Height L1	152	18	0	22	112		
Height L2	55	33	16	6	0		
Height L3	19.5	14	0	5.5	0		
Height L4	7	7	0	0	0		
Modelled	FA total	FA order 1	FA order 2	FA order 3	FA order 4		
Height L1	118	6	0	37	75		
Height L2	20	6	8	6	0		
Height L3	9	4	5	0	0		
Height L4	0	0	0	0	0		
Box13							
Measured	FA total	FA order 1	FA order 2	FA order 3	FA order 4	FA order 5	FA order 6
Height L1	132	28	18	8	26	20	32
Height L2	97	24	17	0	0	22	34
Height L3	138	40	7	46	13	32	0
Height L4	108	62	6	28	12	0	0
Modelled	FA total	FA order 1	FA order 2	FA order 3	FA order 4	FA order 5	FA order 6
Height L1	81	7	13	8	0	20	33
Height L2	66	8	7	0	0	21	30
Height L3	85	0	14	30	26	15	0
Height L4	40	9	6	25	0	0	0

Box25							
Measured	FA total	FA order 1	FA order 2	FA order 3	FA order 4	FA order 5	FA order 6
Height L1	146	53	11	8	0	31	43
Height L2	127	35	26	10	14	15	27
Height L3	142	80	42	0	0	20	0
Height L4	43	38	5	0	0	0	0
Modelled	FA total	FA order 1	FA order 2	FA order 3	FA order 4	FA order 5	FA order 6
Height L1	92	24	0	0	13	15	40
Height L2	89	12	15	10	27	25	0
Height L3	87	40	28	0	0	19	0
Height L4	10	10	0	0	0	0	0

Figure C.2. Frontal area at a certain height occupied by branches of various orders for 10 mangroves.

D. Hand measurement

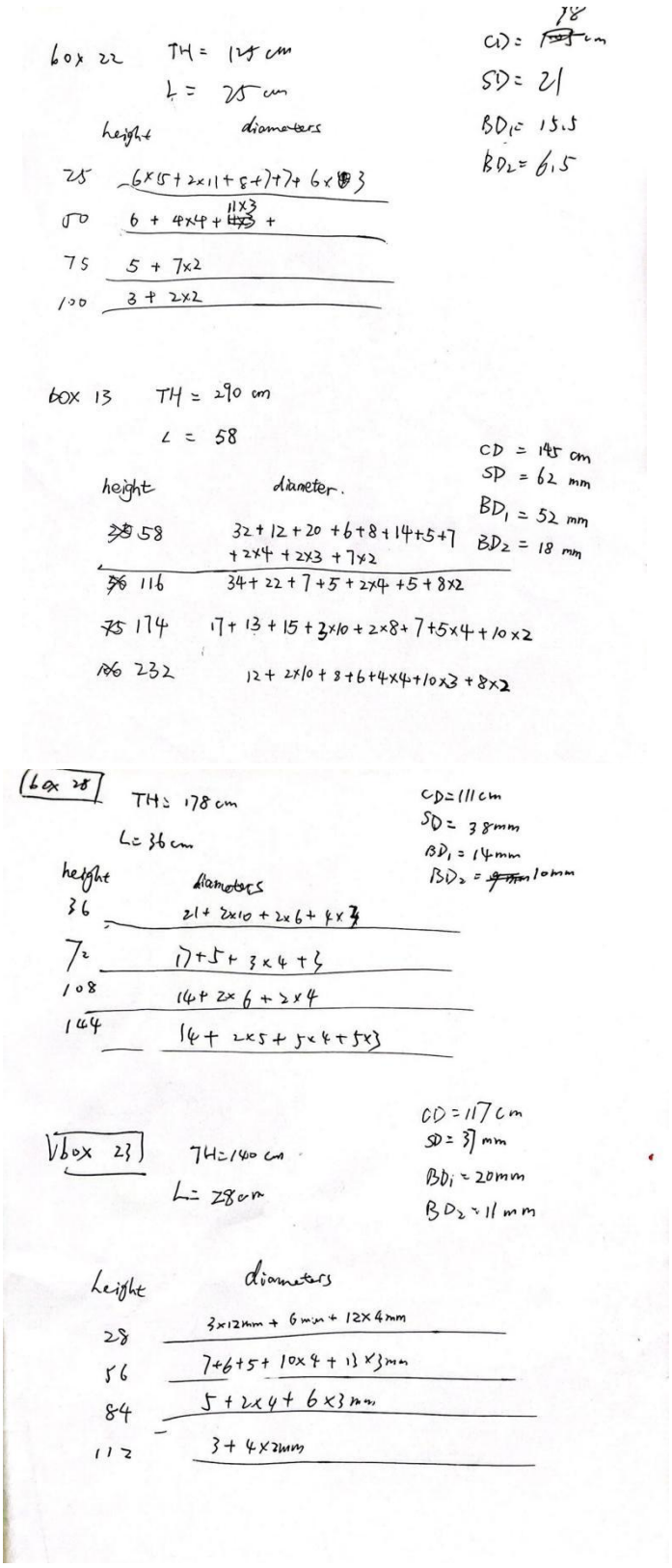

Figure D.1. Part of hand measured results.